

Review

Open Access



PGM-free carbon-based catalysts for the electrocatalytic oxygen reduction reaction: active sites and activity enhancement

Kai Wei¹, Xian Wang^{1,*}, Junjie Ge^{1,2,*}

¹School of Chemistry and Materials Science, University of Science and Technology of China, Hefei 230026 Anhui, China.

²Dalian National Laboratory for Clean Energy, Dalian 116023, Liaoning, China.

*Correspondence to: Dr. Xian Wang, School of Chemistry and Materials Science, University of Science and Technology of China, Hefei 230026 Anhui, China. E-mail: xwang18@mail.ustc.edu.cn; Prof. Junjie Ge, School of Chemistry and Materials Science, University of Science and Technology of China, Hefei 230026 Anhui, China; Dalian National Laboratory for Clean Energy, Dalian 116023, Liaoning, China. E-mail: gejunjie@ustc.edu.cn

How to cite this article: Wei K, Wang X, Ge J. PGM-free carbon-based catalysts for the electrocatalytic oxygen reduction reaction: active sites and activity enhancement. *Energy Mater* 2023;3:300051. <https://dx.doi.org/10.20517/energymater.2023.52>

Received: 4 Jul 2023 **First Decision:** 21 Jul 2023 **Revised:** 25 Jul 2023 **Accepted:** 7 Aug 2023 **Published:** 7 Nov 2023

Academic Editor: Hao Liu **Copy Editor:** Fangling Lan **Production Editor:** Fangling Lan

Abstract

Exploring high-activity, low-cost platinum group metal-free (PGM-free) oxygen reduction reaction (ORR) electrocatalysts to replace precious metal Pt is critical for large-scale fuel cell applications. Owing to their wide source, controllable composition, low price, and excellent performance, the PGM-free carbon-based electrocatalysts have attracted great interest in academia and are expected to be an ideal replacement for precious metal electrocatalysts. In this review, we mainly focus on PGM-free carbon-based electrocatalysts and first introduce the ORR mechanisms and the active site classification of PGM-free carbon-based electrocatalysts. Then, we propose four strategies to enhance the ORR activity of electrocatalysts from the active site perspective based on the relationship between the structure and function of active sites. Finally, we present the current challenges and prospects for developing ORR electrocatalysts exhibiting high performance and stability.

Keywords: Carbon-based electrocatalysts, oxygen reduction reaction mechanisms, active sites, activity enhancement strategy



© The Author(s) 2023. **Open Access** This article is licensed under a Creative Commons Attribution 4.0 International License (<https://creativecommons.org/licenses/by/4.0/>), which permits unrestricted use, sharing, adaptation, distribution and reproduction in any medium or format, for any purpose, even commercially, as long as you give appropriate credit to the original author(s) and the source, provide a link to the Creative Commons license, and indicate if changes were made.



INTRODUCTION

The exploitation of substitute energy sources and new energy conversion equipment has become a growing focus of scientific research, and hydrogen energy is emerging as a recognized low and zero carbon energy source, with proton-exchange-membrane fuel cells (PEMFCs) attracting widespread concern due to their high performance, high energy density, wide range of applications, and low pollutant emissions^[1-6]. In PEMFCs, the conversion of the high energy of hydrogen fuel to electricity is achieved by two chemical processes, the hydrogen oxidation reaction (HOR) and oxygen reduction reaction (ORR), respectively. HOR occurs at the anode, and this reaction requires only a small amount of catalyst due to its fast kinetics. ORR happens at the cathode, and slower kinetics of this reaction results in an overpotential loss approximately ten times greater than that of HOR, requiring high content and expense of platinum group metal (PGM) catalysts, thus limiting performance and large-scale commercial application of PEMFCs^[7-9].

Based on data from the US Department of Energy, at 500,000 fuel cell systems per year, approximately 42% of the total expense is derived from the use of platinum catalysts, and approximately 80%-90% of the platinum catalysts are utilized as cathode ORR electrocatalysts^[1,10,11]. Thus, the exploitation of cost-effective, high-performance, and high-stability PGM-free electrocatalysts to reduce or move away from dependence on precious metals plays a decisive role in achieving sustainable development and large-scale application of PEMFCs^[7,12,13]. Recently, extensive studies have focused on PGM-free ORR catalysts, including carbon-based materials^[14-16], single-atom catalysts^[17-19], transition metal oxides^[20], transition metal nitrides^[11], transition metal sulfides^[21,22], and transition metal phosphides catalysts^[23]. In 1964, Jasinski first reported that phthalocyanine compounds with the Metal-N₄ structure have ORR activity in alkaline media, which broke new ground for PGM-free ORR catalysts^[24]. Within the PGM-free catalysts, carbon-based catalysts offer the benefits of environmental friendliness, less heavy metal contamination, and low cost. Carbon-based materials display tremendous promise in ORR electrocatalysts due to the cheap and easy accessibility of carbon and their desirable electrical/thermal conductivity and adjustability of structure and performance^[25,26]. Carbon-based ORR electrocatalysts are usually classified into transition metal-doped carbon-based electrocatalysts and non-metallic heteroatom-doped carbon-based electrocatalysts according to the doping atoms or active center structure. For example, Fe-N-C catalysts currently show ORR activities close to those of PGM catalysts and high stability, which is expected to significantly decrease the overall costs of PEMFC technology^[27-31].

Currently, there are a number of studies dedicated to enhancing ORR activity of carbon-based electrocatalysts, exploring many strategies to create effective catalytic sites and enhance their stability through physical and chemical strategies. However, modulating the catalytic behavior of carbon-based electrocatalysts is hampered by the lack of insight into the active site structure and a catalytic mechanism that regulates the inherent ORR activity, which would hinder the development of activity and stability of carbon-based electrocatalysts. As excellent performance clearly depends on active centers of electrocatalysts, determining the active site structure is essential for understanding and improving ORR activity of carbon-based electrocatalysts and designing carbon-based electrocatalysts^[32,33].

In this review, we concentrate on ORR mechanisms and the active site structure of carbon-based catalysts and analyze effective strategies to boost ORR performance of carbon-based electrocatalysts from the active site perspective after recognizing and understanding these active sites [Figure 1]. With this knowledge, we can identify the interconnection of active site structures and functions to drive exploitation of carbon-based PGM-free electrocatalysts and offer personal insights.

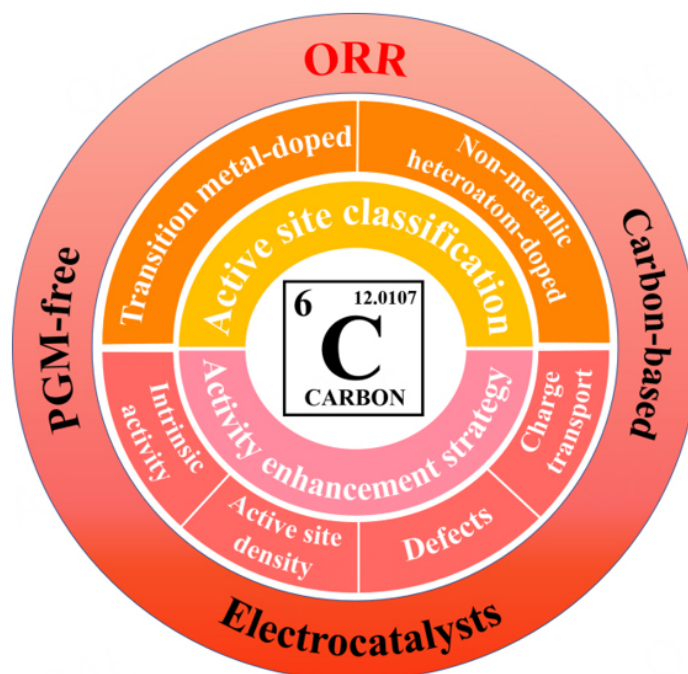


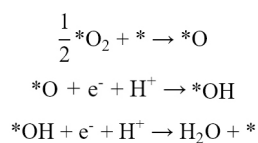
Figure 1. Schematic of major overview content of carbon-based ORR electrocatalysts.

ORR MECHANISMS

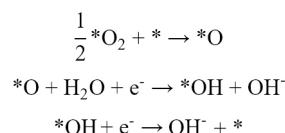
ORR is the most significant multi-electron process in PEMFCs, with mainly oxygen molecules (O_2) gaining electrons in the acidic or basic medium at a cathode to yield a series of oxygen-containing substances^[34,35]. The ground state of oxygen is the paramagnetic triplet oxygen (3O_2), which is usually less reactive than the diamagnetic and unstable singlet state (1O_2)^[36-38]. The reaction of 3O_2 with catalysts usually occurs in two steps, weakening O-O bond and interconverting the spins of the unpaired electrons to complete the conversion. Among them, spin inversion is considered the more complex task due to its extremely slow reactivity. Interestingly, when 3O_2 reacts with a material having unpaired electrons (the catalysts mentioned in this paper), a spin restriction is eliminated or becomes negligible so that the O-O bond remains intact in the first step and breaks in subsequent reaction steps^[39,40]. For brevity, the latter is described using O_2 instead of 3O_2 . ORR is classified into three categories according to the order of O-O bond breakage, i.e., dissociative pathway, associative pathway, and peroxide pathway. These three mechanisms follow the following formula:

(i) The dissociative pathway (step 1)

In the acid medium:

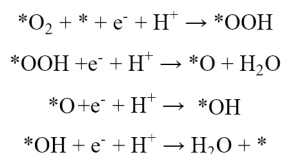


In the basic medium:

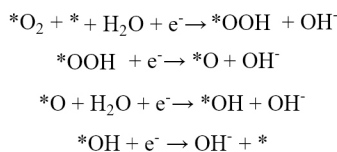


(ii) The associative pathway (step 2)

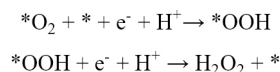
In the acid medium:



In the basic medium:



(iii) The peroxide pathway (step 3)



where * represents catalytic activity centers.

Regarding the ORR mechanism, first, O_2 molecules diffuse from the solution proper to the catalyst surface to form adsorbed O_2 molecules ($*O_2$), and subsequently, $*O_2$ undergoes several reduction pathways, as described above. Step 1 is one in which O-O bond breaks straight after activation of oxygen on the catalyst to form $*O$, which is then sequentially protonated and reduced to $*OH$ and H_2O . Step 2 is one in which $*O_2$ first becomes $*OOH$, followed by the production of $*O$ and $*OH$ intermediates by breaking the O-O bond. Step 3 is the sequential reduction of $*O_2$ intermediates to $*OOH$ and H_2O_2 before O-O bond is broken. In general, step 1 and step 2 are the most promising four-electron reaction pathways for ORR, and they differ in whether the chemisorbed O_2 dissociates before or after protonation^[41]. The four-electron reaction pathway possesses faster reaction kinetics and improves energy conversion efficiency, which is an ideal ORR reaction pathway. It is worth noting that step 3 has slow reaction kinetics. The H_2O_2 intermediate produced by this pathway oxidizes/corrodes the active site and the carbon carrier. It also resists complete reduction, which has a significant effect on the activity and stability of the ORR electrocatalyst. Additionally, this phenomenon accounts for the low current efficiency^[42,43]. In PEMFCs, H_2O_2 can damage Nafion membranes and cause a decrease in ORR performance, leading to a corrosive effect of its decomposition into highly reactive intermediates. It has been demonstrated that more H_2O_2 is generated on PGM-free electrocatalysts compared to PGM electrocatalysts, which is most probably attributed to the poor catalytic activity of active sites for O-O bond breakage, which occurs after proton and electron transitions^[44]. For transition metal

carbon-based electrocatalysts, the degradation of active centers by H_2O_2 is one of the key issues affecting the stability of this type of catalyst^[45]. Therefore, the concept of ORR catalysts following a four-electron pathway instead of a two-electron pathway would be a promising idea for designing highly active and stable electrocatalysts.

Various oxygen-containing species (e.g., $^*\text{O}_2$, $^*\text{O}$, $^*\text{OH}$, $^*\text{OOH}$) are involved in ORR, and their adsorption strengths are critical to the electrocatalysis^[46]. The adsorption strength of $^*\text{O}_2$ generated by O_2 adsorption on the catalyst will directly affect the breakage of O-O bond and ease of their desorption. Excessive adsorption strength, on the one hand, increases the adsorption of O_2 by the catalyst and the generation of intermediates; on the other hand, it causes difficulties in the desorption of oxygen species and will affect the subsequent radical reactions and thus, the ORR rate and activity, which are explained by interactions of oxygen-containing species with the active site through oxygen terminus, which is consistent with $^*\text{O}_2$. And excessively weak adsorption strength prevents the transfer of protons and electrons to oxygen-containing species. By promoting and balancing the adsorption and desorption of O_2 and its oxygen-containing species, it is possible to exchange O_2 efficiently and reduce the reaction resistance, as well as to improve the diffusion-limited current density and kinetic current, which are intimately associated with the ORR performance^[47]. Therefore, theoretical calculations are often employed to investigate the correlation between the adsorption strength of oxygen-containing species and ORR activity. Since the interaction between oxygenated species and active sites is similar to that of O_2 , a linear correlation of scaling relationship (SR) is found among adsorption energy of each oxygenated species. The SR is $\Delta E_2 = A\Delta E_1 + B$, where ΔE_1 and ΔE_2 are adsorption energy of different oxygen-containing species, A and B are constants for different oxygen-containing species 1 and 2 at a given adsorption site, respectively^[48]. The SR makes it possible to describe the adsorption capacities of all intermediates and products by employing only one adsorbent. The association between the adsorption strength of oxygen-containing species and ORR catalytic activity is understood by Sabatier's rule, which stipulates the existence of an appropriate interaction between each species and the catalyst surface to attain optimal ORR performance^[41]. Furthermore, adsorption energy of oxygen-containing species can roughly determine reaction pathways in which ORR occurs. Low adsorption energy is not favorable for breaking O-O bond and facilitates the development of a two-electron reaction, while high adsorption energy, on the other hand, favors the four-electron pathway.

Quantum spin exchange interaction (QSEI) is one of the decisive electronic factors that predispose the active site to optimally bind adsorbed oxygen atoms for catalytic activity^[49,50]. The vast majority of catalysts mentioned later have unpaired electrons in open-shell electronic configurations, which implies that QSEI can accelerate the catalysis of ORR. A QSEI effect remarkably influences bonding and activation enthalpies during chemical reactions, and hence ORR reaction rate and activity^[51]. Great charge transport, moderate adsorption of oxygen-containing intermediates, and spin-selectivity are the keys to ORR performance enhancement.

In summary, an in-depth study of ORR mechanisms is essential for understanding, designing, and improving ORR electrocatalysts and also for improving the stability of electrocatalysts by reducing the production of H_2O_2 through modulating the adsorption energy with the help of theoretical calculations.

PGM-FREE CARBON-BASED ELECTROCATALYSTS: ACTIVE SITES

The doping of various types of atoms, such as transition metal atoms and inorganic non-metal atoms, in the carbon skeleton will more or less enhance the catalytic activity, which is essentially based on active sites. Generally, catalyst surface atoms in active sites have greater catalytic activity than the other atoms on the specific surface sites. Understanding and appreciating active sites of carbon-based electrocatalysts may

contribute to the design of catalysts to enhance their catalytic activity and stability, such as modifying specific active sites to increase their corrosion resistance to electrolytes for enhanced stability. There are two types of carbon-based PGM-free electrocatalysts, and this section will focus on the active site types of these two types of electrocatalysts for a detailed discussion.

Transition metal-doped carbon-based electrocatalysts

For a traditional transition metal/nitrogen-doped carbon (M-N-C) catalyst, the single transition metal atom in the same plane is coordinated with the adjacent atoms, typically nitrogen (N) atoms, forming the MN_x structure. The MN_x site and the carbon skeleton synergize with each other to complete the ORR. The former interacts with the ORR reactants as the active site, while the latter provides a pathway for mass transportation by virtue of its high specific surface area, high electrical conductivity, and large pore volume^[52]. M-N-C catalysts possess abundant active sites that reduce the energy potential barrier of oxygen-containing species and are the most prospective candidate catalysts, especially the Fe-N-C catalysts that are comparable to PGM catalysts to a certain extent. M-N-C catalyst sites are classified into central metal atom sites, MN_x sites, N-C sites, and crystallized iron and species, and we concentrate on Fe-N-C electrocatalysts, which have the highest research potential at present.

Central metal atom sites

For ORR, central metal atoms are thought to be active sites for O_2 adsorption and subsequent electron transfer, which is attributed to the d orbitals of the central metal atom interacting with the p electrons of O_2 and oxygen-containing species^[53,54]. Consequently, the chemical property of central metal atoms plays an important role in the determination of ORR electrocatalytic activity of M-N-C electrocatalysts. Early studies revealed that modulation of ORR activity by metal atomic centers in M-N-C electrocatalysts (M = Fe, Co, Ni, Cu, and Mn) was understood in terms of molecular orbital (MO) theory, and results showed ORR activity with a tendency of $Fe > Co > Ni > Cu \cong Mn$ ^[55]. In recent years, Zheng *et al.* demonstrated that the central metal atom ($Fe > Co > Mn > Ni$) has a close relationship with ORR activity of M-N-C catalysts [Figure 2A]^[56]. We can see from Figure 2B and C that different central metal atoms have variable tendencies to catalyze the ORR pathway, and the two-electron reaction pathway produces more HO_2 , reducing the electron transmission efficiency and consequently lowering the activity of the ORR. Moreover, ORR activity of active centers with various central metal atoms was systematically calculated by Zheng *et al.* [Figure 2D]^[56]. It is possible to observe that the right sides of two volcano curves almost overlap, suggesting that the two curves are both defined by the original OOH generation stage in the weakly bound area. Instead, the left sides of U_1 and U_2 are defined by removal steps of OH and OOH species, respectively. Therefore, catalysts with high U_1 vs. low U_2 are desired, corresponding to a high four-electron reaction tendency and a low two-electron reaction tendency. Figure 2E demonstrates the sequence of ORR activity of M-N-C electrocatalysts similar to experimental results. As shown in Figure 2F, Peng *et al.* obtained similar findings for the central metal atom ($Fe > Co > Cu > Mn > Ni$)^[57]. This study indicates that the results apply to both basic and acidic mediums, with the difference in performance being more pronounced in acidic electrolytes. Furthermore, Venegas *et al.* demonstrated that M(III)/(II) redox potential is the reactivity descriptor for the ORR of M-N-C catalysts and M(II) is the major active site, which applies to M-N-C catalysts derived from pyrolysis of macrocyclic compounds^[58]. They further proposed two diverse mechanisms targeting M(II)- O_2 binding energy and the redox potential of the catalysts. The results revealed that the more positive the redox potential of central metal atoms, the stronger the ORR catalytic performance, which is explained by the reduction of basicity of the ligand around MN_x after the pyrolysis of the macrocyclic compound, resulting in a stronger electron absorption capacity^[59]. The central metal atom as the active center for O_2 adsorption is critical for ORR performance^[60]. M-N-C electrocatalysts with weak adsorption capacity for oxygen have difficulty in breaking O-O bond of $*OOH$ and O_2 , and a two-electron

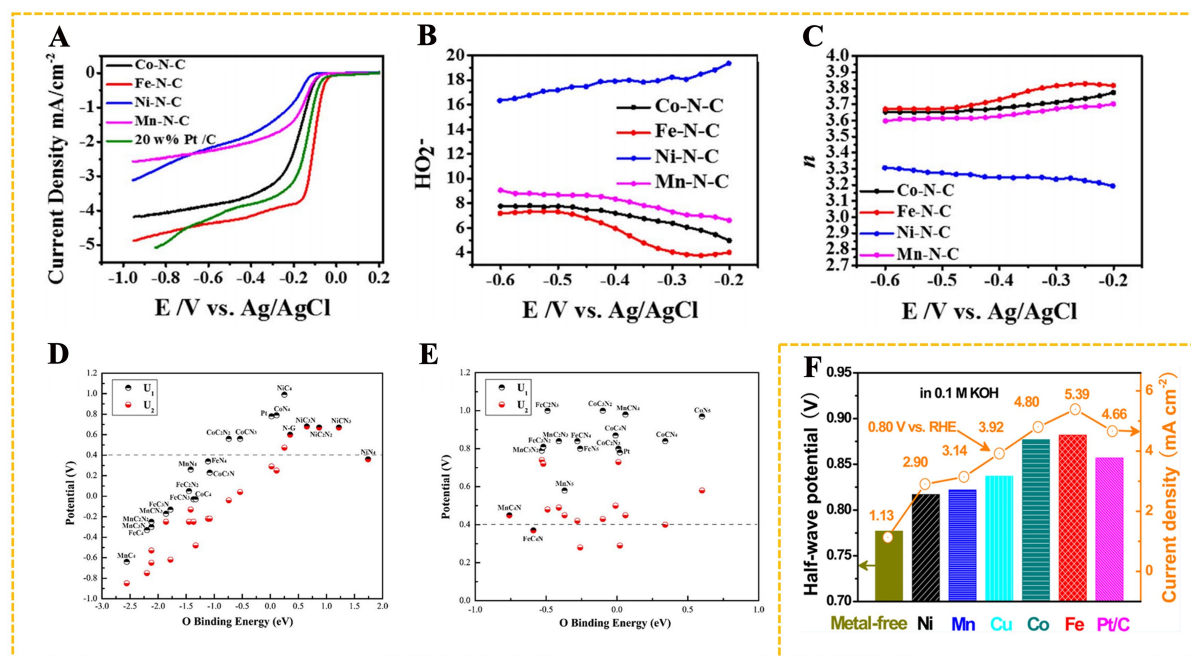


Figure 2. (A) LSV curves of Pt/C and M-N-C. (B) Percentage of HO₂⁻ productivity of M-N-C. (C) Numbers of electron transference of M-N-C. (D) The U₁ and U₂ on various square planar active sites are graphed as a function of O binding energy, where the U₁ represents the potential for four-electron ORR and U₂ for two-electron ORR. (E) U₁ and U₂ of the ORR procedure are graphed as a function of O binding energy on metal centers of all possible square pyramids, producing a high active plateau area, while the medium binding energy is about 0 eV. Reproduced from Zheng *et al.*^[56] by permission from Elsevier. (F) E_{1/2} of M-N-C electrocatalysts based on various metals were tested by LSV. Reproduced from Peng *et al.*^[57] by permission from the American Chemical Society.

reaction tendency in ORR increases and generates more H₂O₂, such as Ni-N-C catalysts. M-N-C catalysts with strong adsorption ability to oxygen are easy to O-O bond breaking and proton/electron transference and mainly carry out a four-electron reaction pathway in ORR, such as Fe-N-C electrocatalysts of excellent ORR performance.

To sum up, transition PGM-free, such as Fe, Co, Mn, and Ni, are critical to ORR activity of M-N-C electrocatalysts, and their species significantly affect the performance of PEMFCs. Fe-N-C electrocatalysts have a high capacity for O₂ adsorption and follow mainly the four-electron reaction pathway with an optimal ORR performance that is steadily approaching commercial Pt/C. However, stability is one of the major factors hindering their application. Fe-N-C electrocatalysts tend to form Fenton reagents through the reaction of H₂O₂ with Fe(III)/(II), and the generation of strong oxidative radicals may damage ionic cross-linked polymers and proton exchange membranes, compromising the fuel cell lifetime. As mentioned previously, modification of specific active sites is expected to improve the stability of Fe-N-C catalysts. For example, Shen *et al.* developed the template casting methodology to form a thiophene-like structure (C-S-C) by doping S in Fe-N-C, which reduced the electron localization around Fe active sites, allowing the active site to interact strongly with *O₂ and *OOH, improving four-electron reaction selectivity of the catalyst while reducing the production of H₂O₂^[61]. By studying the relationship between Fe-N bond energy and temperature, Li *et al.* found that the Fe-N bond energy was highest at 700 °C, and further rises in temperature would lead to nitrogen shedding, resulting in reduced activity and stability^[62]. Therefore, improving the stability of the catalyst can be started from the Fe-N bond energy in FeN₄ sites. Co-N-C electrocatalysts are an ideal choice with less hazardous Fenton reaction, but they move toward more two-electron reaction pathways in acidic media, generating undesired H₂O₂, which may also impair the performance of PEMFCs, hindering commercial application. Mn-N-C electrocatalysts have excellent

stability due to their specificity for four-electron reaction pathways, thus avoiding the Fenton reaction, but their inherent ORR activity is relatively poor. Additionally, their research and development are still in the early stages. Ni-N-C electrocatalysts have the lowest intrinsic ORR activity due to their tendency to follow a two-electron reaction pathway, which generates more HO_2^- and reduces the ORR activity. Moreover, it has been found that Ni-containing groups in Ni-N-C catalysts have a toxic influence on ORR activity, and the existence of Ni has a degenerative impact on the catalytic current^[60].

M-N_x sites

This section introduces the M-N_x site as an example of Fe-N-C electrocatalysts. In theory, the FeN_x site can have six coordination patterns (e.g., FeN₁, FeN₂, FeN₃, FeN₄, FeN₅, and FeN₆) [Figure 3]. Li *et al.* prepared the FeNC-300 catalyst using ZIF-8 as the precursor at 300 °C. They adopted a combined experimental and theoretical method to confirm that the active site is FeN₁, but the FeN₁ site has poor ORR activity^[63]. Zhu *et al.* developed a synthetic strategy based on the bimodal template to prepare graded porous Fe-N-C catalysts with FeN₂ sites with a half-wave potential of 0.927 V^[64]. This potential is 55 mV higher than that of commercial Pt/C, and the catalyst possesses excellent ORR performance in alkaline medium^[64]. Kabir *et al.* investigated that FeN₃ based on double carbon vacancy defects (DV-FeN₃/C) possesses promising formation energy and could be formed during high-temperature synthesis^[65]. However, FeN₃ sites are generally not desirable for ORR catalysts due to their high ORR resistance^[66]. Wang *et al.* demonstrated the satisfactory design and preparation of porous Fe-N-C catalysts using directly pyrolyzed mixtures of iron-containing zeolite imidazolium framework-8 precursors and NaCl^[28]. These catalysts show outstanding ORR electrocatalytic activity in alkaline solutions owing to their distorted FeN₄ sites^[28]. Huang *et al.* achieved fabrication of a suitable three-dimensional (3D) graphene aerogel-supported FeN₅ section^[67]. The axial substrate markedly altered the electronic and geometry structure of iron centers in FeN₅ sections, and the catalyst displayed great ORR activity and stability^[67]. Besides, three Fe/N/S (sulfur) modified carbon electrocatalysts were prepared by Zhu *et al.* employing pyrolytic polymerization^[68]. They affirmed that the FeN₆ structure, which was a Fe(III) complex with six coordination sites [FeN₆, Fe(III)(porphyrin)(pyridine)₂], was true active sites of the ORR by applying sophisticated electron microscopy and Mössbauer spectroscopy. To conclude, FeN₁ and FeN₃ are restricted in PEMFCs due to their high ORR resistance. FeN₅ and FeN₆ have been less investigated due to the complexity of preparing pure products despite their considerable ORR activity and satisfactory durability. Currently, there is a large amount of literature reporting FeN₄ as the main active site in Fe-N-C electrocatalysts^[69,70]. Nevertheless, some previous theoretical and experimental results suggest that FeN₂ structures have higher ORR activity than that of FeN₄ and are ideal active sites for M-N-C electrocatalysts^[61,71]. Therefore, we will focus our discussion on these two active sites in the following.

In response to the question of whether FeN₂ or FeN₄ is the optimal active site, some scholars consider FeN₂ to be the optimal active site. Song *et al.* adopted the density functional theory (DFT) to predict that FeN₄ is not the optimal active site due to its strong interactions with oxygen-containing intermediates^[72]. They used both theoretical and experimental methods to reveal the relationship between the activity of various active sites on ORR: FeN₂ > FeN₄ > Fe₄N > NC > Fe₄C ≥ C. They synthesized Fe-N-C electrocatalysts with FeN₂ as active sites based on the ease with which carbon black can be oxidized by nitric acid. The optimal activity of FeN₂ was derived from its sitting at the edge of graphene, which facilitates O-O bond breakage for O₂ adsorption. Lefèvre *et al.* studied the active sites of Fe-N-C catalysts, employing time-of-flight secondary ion mass spectrometry (TOF-SIMS)^[73]. They discovered that FeN₂ and FeN₄ were co-existing in the catalysts and that FeN₂ had superior electrocatalytic activity than FeN₄, while the FeN₂ content was related to the iron precursor and the pyrolysis temperature during fabrication, and the FeN₂ content could be tuned to its maximum value to gain optimal ORR activity. Shen *et al.* proposed the fabrication of a porous carbon

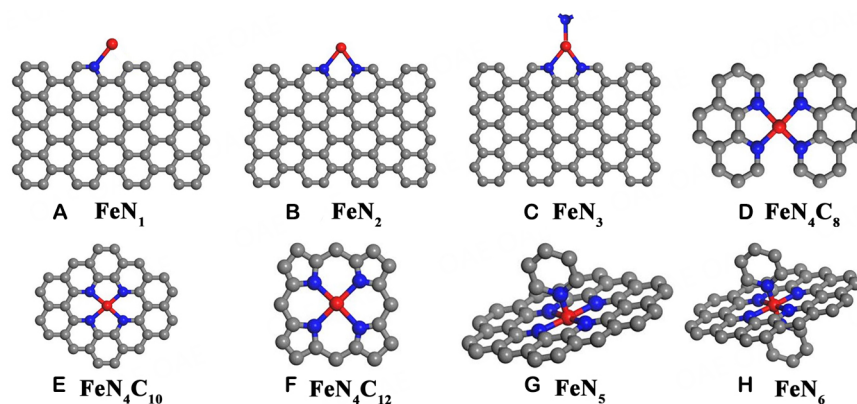


Figure 3. Coordination structures of Fe-N-C electrocatalysts, where the red spheres, blue spheres, and gray spheres correspond to iron, nitrogen, and carbon, respectively.

material with highly atomically dispersed FeN_2 sites, which displayed excellent ORR activity^[71]. In addition, numerous scholars have concluded that FeN_x is the best active site of ORR. Kabir *et al.* derived the results of Fe-N-C electrocatalysts with multiple defects during the pyrolysis through DFT calculations and X-ray photoelectron spectroscopy (XPS) tests^[65]. The defect abundance is dependent on the order of formation energy as follows: $\text{FeN}_4 > \text{FeN}_3 > \text{FeN}_2$ ^[65]. The relationship between FeN_x active sites and ORR activity was systematically investigated by Li *et al.* through DFT calculations^[63]. From **Figure 4A**, it can be observed that various active sites have a “volcanic” relationship with ORR activity and an “anti-volcanic” relationship with their formation energies. It is noted that higher heat treatment temperatures contribute to the formation of more stable structures with lower formation energies, and in their experiments, FeN_4 was formed at a maximum temperature of 1,000 °C with exceptional ORR activity and stability. The FeN_x structure is controversial owing to the differences in catalyst ORR performance caused by factors such as the unknown mechanism of pyrolysis of carbon-based catalysts, different preparation methods, and research tools, but the FeN_4 structure is undoubtedly and widely recognized as the high ORR active site. Based on the number of surrounding carbon atoms, FeN_4 sites were further subdivided into various configurations involving FeN_4C_8 , $\text{FeN}_4\text{C}_{10}$, and $\text{FeN}_4\text{C}_{12}$ [**Figure 3D-F**]. Li *et al.* revealed two types of FeN_4 sites by combined operation of Fe Mössbauer spectroscopy and X-ray absorption spectroscopy (XAS): the high-spin $\text{FeN}_4\text{C}_{12}$ moiety (S1) and the low- or medium-spin $\text{FeN}_4\text{C}_{10}$ moiety (S2)^[74]. Both sites originally made contributions to the ORR activity, yet as the time of reaction continued, the S1 sites with higher intrinsic activity were rapidly transformed into inactive Fe_2O_3 and degraded, while the number and structure of S2 sites embedded in the compact carbon planes remained unchanged [**Figure 4B**]^[75]. This research offers directions for enhancing the mass activity and stability of electrocatalysts, i.e., increasing densities of stable S2 sites. In addition, Xu *et al.* found that the rapid decrease in catalyst ORR activity in the initial stage was probably due to the demetalization of the unstable FeN_4C_8 site, and the maintenance of more stable properties in the later stage may be attributed to $\text{FeN}_4\text{C}_{12}$, which is consistent with the study of Xu *et al.*^[76].

Furthermore, the chemical environment of FeN_4 can remarkably influence ORR activity. Liu *et al.* demonstrated two FeN_4 sites in Fe-N-C electrocatalysts, a highly active S1 site with four pyrrole-type N ligands and a highly stable S2 site with four pyridine-type N ligands, respectively^[77]. They employed the DFT theory to clarify the effect of ligand structures on ORR activity. They discovered Fe in the S2 site has more vacant d orbitals, which have greater adsorption to O_2 , resulting in hard O-O bond dissociation and, therefore, low activity of the pyrrole-type FeN_4 site [**Figure 4C**]^[77]. Yang *et al.* also showed that ORR activity of pyrrole-type sites is superior to that of pyridyl-type sites. They pointed out that the Fe atom in the pyrrole-type site triggers the activation of eight carbon atoms neighboring pyrrole-N atoms as extra ORR

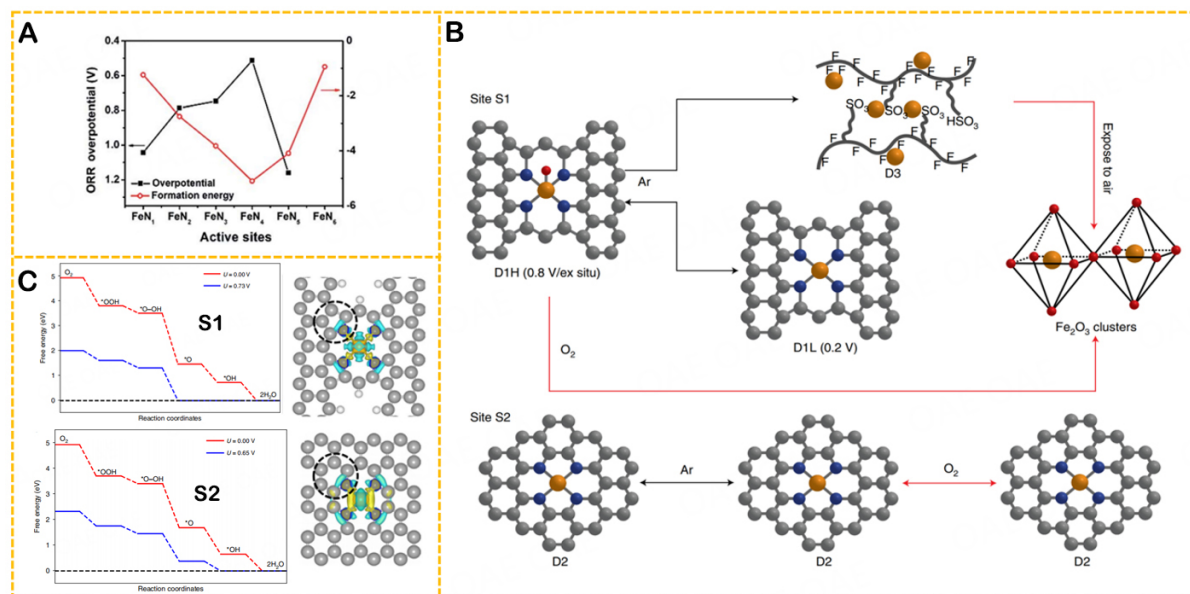


Figure 4. (A) The ORR overpotentials of FeN_x and the formation energies of FeN_x were calculated by DFT. Reproduced from Li *et al.*^[63] by permission from the Royal Society of Chemistry (RSC). (B) Schematic diagram of structural variations of S1 and S2 sites. The highly reactive and low-stability S1 site rapidly transforms to inactive iron oxide. On the contrary, the low-activity and high-stability S2 sites are critical for maintaining fuel cell performance late. Reproduced from Li *et al.*^[74] by permission from the Springer Nature. (C) The activity of both kinds of FeN₄ sites was calculated with DFT. Reproduced from Liu *et al.*^[77] by permission from the Springer Nature.

active sites^[78]. When the FeN₄ site is situated at the boundary of a carbon plane, such as the edge of graphene micropores, the ORR activity of such sites is greater, which is due to band gap shrinkage and local electron redistribution^[79,80]. Fu *et al.* synthesized Fe-N-C catalysts by edge-engineering via an NH₄Cl-assisted method^[81]. DFT calculations revealed that FeN₄ sites with neighboring pore defects possess higher ORR intrinsic activity than non-defective configurations. Moreover, Mineva *et al.* coupled DFT with Mössbauer spectroscopy to identify the existence of two states of FeN_x sites: low-spin Fe(II) and high-spin Fe(III) states, while a few sites may be present in the Fe(II) ($S = 1$) state. This study shows that D2 (Fe(II)N₄C₁₀ sites in low and medium spin) may not be able to bind with O₂ or its ability to bind with O₂ is weaker than that of D1 (Fe(III)N₄C₁₂ sites in high spin). In contrast, D1 is more easily produced on the surface and is the main active site^[82].

In summary, the electronic structure of the MN_x site can be changed via adjustments to the type, structure, and chemical environment (edge effect, spin type, *etc.*) of the ligand N atom, especially for the d electrons of central metal atoms, and they will greatly enhance the electrocatalytic activity of the ORR.

N-C sites

Numerous studies have indicated that metal species are only involved in catalyzing the generation of ORR active carbon structures without constituting active sites and that existence of metal substances facilitates the integration of N atoms to carbon materials and contributes to the formation of N-C sites (graphitic N (GNG), pyridinic N, and pyrrolic N)^[83,84]. N atoms with stronger electron acceptability and higher electronegativity than carbon atoms can activate carbon pi electrons, thus disrupting the integrity of the pi-conjugated system and inducing charge redistribution, which increases the electronic characteristics of the catalyst and enhances ORR performance^[85]. Artyushkova *et al.* showed that pyrrole N facilitates the catalytic two-electron reaction, resulting in more H₂O₂, while pyridine N (PNG) catalyzes the second stage of H₂O₂ reduction or catalyzes the direct reduction of O₂ to H₂O and is an ideal ORR active site^[86]. Parvez *et al.*

investigated using amino cyanine as a nitrogen source and graphene oxide as a precursor, followed by the doping of iron nanoparticles to form electrocatalysts with better ORR activity than Pt electrocatalysts, showing GNG is an effective active site^[87]. Numerous studies have suggested that exposed nitrogen species will influence the adsorption and activation of O₂ and formation of other oxygen-containing species^[88]. Lai *et al.* demonstrated that ORR performance was closely related to graphite N content, and graphene N can significantly improve the limiting current density^[89]. In addition, PNG facilitates the enhancement of the ORR onset potential, thus shifting the ORR tendency from a two-electron reaction to a four-electron reaction^[89]. Cui *et al.* prepared iron-containing PNG-dominated graphene aerogels and proved that the concerted action of PNG and FeN_x enabled the catalyst to display exceptional ORR activity^[90]. Huang *et al.* developed a Fe/Fe₃O₄@N-G electrocatalyst that outperformed Pt/C catalysts with outstanding ORR performance because of chemical composition of metal agglomerates and high PNG dopants^[91].

To sum up, a N-C site is beneficial for improving ORR activity owing to the high electronegativity and strong electron-accepting ability of the N atom, which makes the active nitrogen species positively charged and influences the ORR process. PNG and graphite N are more desirable ORR active sites, which is attributed to their increased onset potential and limiting current density. In contrast, pyrrole N should be diminished in the design of ORR electrocatalysts due to its strong catalytic effect on the two-electron ORR pathway to avoid undesirable H₂O₂ by-product generation, which affects the subsequent ORR process. In addition, a purposeful increase in PNG content also facilitates ORR toward the four-electron reaction pathway.

Crystallized iron species

As other catalytic species or several active sites are inevitably introduced during pyrolytic synthesis at high temperatures^[92,93], up to now, numerous research works have found that crystalline iron species are useful ORR active sites. Faubert *et al.* found that Fe₃C nanoparticles are effective active sites for Fe-N-C catalysts, where carbon shell encapsulates the agglomeration of iron atoms^[94]. The study used X-ray diffraction (XRD) and transmission electron microscope (TEM) to demonstrate that the active site of the catalyst was inorganic and that most of the metal was encapsulated in a carbon-based coating. Varnell *et al.* demonstrated that reversible deactivation and reactivation of Fe-N-C electrocatalysts could be realized with high-temperature Cl₂ and H₂ treatments^[95]. It was shown that carbon-encapsulated Fe nanoparticles are the catalytically active sites for ORR. Choi *et al.* revealed that PNG-coated iron nanoparticles in Fe-N-C electrocatalysts have moderate activity in both direct and indirect ORR four-electron processes^[96]. Qiao *et al.* developed a high-ORR activity FeNC-S-Fe_xC/Fe electrocatalyst, and they employed DFT calculations to indicate that atomically dispersed FeN_x, Fe_xC clusters, and doped S were all active sites, and their interactions act as important in the catalytic activity^[97]. Hu *et al.* proposed that a Fe-N-C catalyst based on graphene layer-encapsulated Fe-/Fe₅C₂ nanoparticles^[98]. The Musburger spectra confirmed that the iron species consisting of Fe and Fe₅C₂ were the main active sites. The electrocatalyst has a favorable ORR in basic solutions with a positive half-wave potential of 20 mV. Wang *et al.* showed that a N-doped porous carbon nanosphere with great ORR performance loaded with Fe₃O₄/Fe₂O₃/Fe nanoparticles^[99]. It was shown that the presence of Fe₂O₃ added to the active site amount enhanced electrolyte diffusion and facilitated oxygen adsorption. The coexistence of Fe₃O₄/Fe₂O₃/Fe significantly increased ORR activity. This research also demonstrates that the synergistic interaction between crystalline iron species enhances the catalytic activity of active sites. Furthermore, researchers have disputed the catalytic role of crystalline iron species in the ORR. Some studies suggest that crystalline iron species are not effective ORR catalytic centers, and they may also inhibit ORR electrocatalytic activity. Kramm *et al.* showed that crystalline iron species removed from electrocatalysts via acid cleaning significantly increased the ORR activity, and they, thus, obtained high concentrations of FeN_x sites, which was owing to the low ORR performance of crystalline iron species and

hindered the exposition of active sites^[100]. Wang *et al.* embedded Fe₃O₄@N-doped-C (Fe₃O₄@NC) nanoparticles in N-doped hierarchical porous carbon to obtain Fe₃O₄@NC/NHPC composites^[101]. The active site probing experiments showed that the contribution of Fe₃O₄ to the ORR performance was very little, and Fe-N_x was critical for the performance enhancement as the main active site^[101]. In addition, they confirmed that Fe₃O₄ has almost no effect on the catalysis by completing removal of iron species using concentrated acid cleaning.

In conclusion, crystalline iron species perform a dual role in Fe-N-C electrocatalysts, acting in one way as active sites to enhance ORR performance while in the other as interferers to cover the active sites and hinder them from performing the catalytic function. The above situation is caused by the fact that the intrinsic relationship between the structure and function of carbon-based electrocatalysts has not been clarified, based on which further development is needed to clarify the role of crystalline iron species in transition metal carbon-based catalysts.

Non-metallic heteroatom-doped carbon-based electrocatalysts

There are numerous studies on doping various heteroatoms (for example, N, B, phosphorus (P), S, and Cl) into carbon materials to show excellent ORR activity. In particular, N doping has become the most widely studied category, dating back to the finding of ORR catalysts made up of N-doped carbon nanotube arrays in 2009, which opened up a wave of research in this area^[102]. Therefore, this paper focuses on N-doped non-metallic carbon-based catalysts to discuss the active sites of heteroatom-doped carbon-based electrocatalysts. There are six types of active sites for N-doped carbon-based electrocatalysts: PNG, pyrrole N, graphite N, oxidized N, sp-hybridized N, and defect sites. In addition, we briefly introduce the active sites of other non-metallic heteroatom-doped carbon-based catalysts.

Non-metallic nitrogen-doped carbon-based catalysts

Nitrogen atoms have similar atomic radii to carbon atoms, which will effectively reduce the lattice mismatch. Moreover, the nitrogen atom, with its large electronegativity, has a lone pair of electrons and one more electron than the carbon atom, which facilitates the occurrence of ORR reactions. Therefore, the N-doped carbon-based electrocatalysts have good ORR activity and stability. There are five main types of doping found in N-doped carbon-based catalysts: PNG, pyrrole N, graphite N, oxidized N, and the recent development of sp-hybridized N [Figure 5A]^[103,104]. Liu *et al.* systematically analyzed the association of structures and activity of various nitrogen-containing active sites on N-doped carbon by combining finely tuned local reaction condition experiments with quantum chemical calculations^[105]. They discovered that the order of various nitrogen-containing sites in ORR: pyridinic N > pyrrolic N > GNG > oxidized N > C (carbon). In addition, it was confirmed that PNG and pyrrole N facilitate the catalytic ORR four-electron reaction, while graphite N and oxidized N facilitate the catalytic ORR two-electron reaction to yield more H₂O₂. Zhao *et al.* proposed a sp-N-doped graphitic electrocatalyst with sp-hybridized N sites^[103]. The greater electronegativity of the sp-hybridized N atom compared to PNG, the more positively charged its adjacent C is, which favors the adsorption of O₂ and improves ORR performance. There are various debates about the contribution of various types of doped N to ORR, and our understanding of this topic is still in its infancy. Some scholars believe that PNG is the primary active site of N-doped carbon-based electrocatalysts and may act in conjunction with pyrrole N. Rao *et al.* fabricated vertically aligned carbon nanotubes (VA-CNTs) with various surface N concentrations using the alumina template technique^[106]. It was discovered that CNT_{PMVD} with a N concentration of 8.4%, displayed the most excellent ORR activity because the material possessed more pyridinic N active sites [Figure 5B]. Li *et al.* prepared 3D flower-shaped N-doped carbon materials using co-pyrolysis of ferrocene and melamine at 500-700 °C^[107]. They found that the material with the highest PNG content (NC-600) outperformed the other catalysts in terms of electron transfer number, half-wave potential, and kinetic current density, suggesting that PNG was the active site of the catalyst

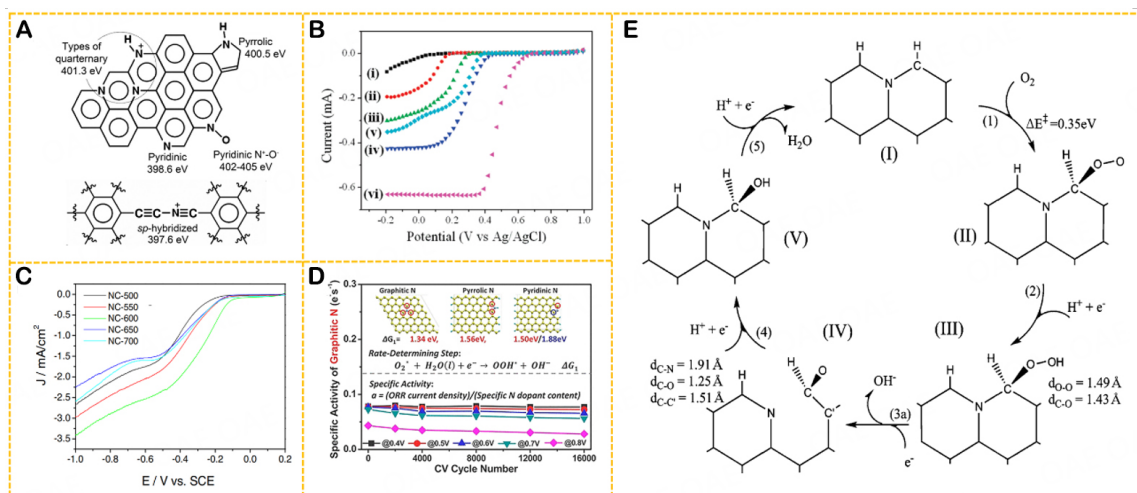


Figure 5. (A) Graphical illustration of typical N species in nitrogen-containing graphitic and corresponding binding energies of XPS as marked. Reproduced from Yang *et al.*^[104] by permission from Wiley-VCH. (B) LSV curves of CNT_{PPA} (i), CNT_{P4VP} (ii), CNT_{PMPy} (iii), CNT_{PMVI} (iv), CNT_{PPP} (v), and Pt/C (vi). Reproduced from Rao *et al.*^[106] by permission from the American Chemical Society (ACS). (C) LSV curves of different NC catalysts. Reproduced from Li *et al.*^[107] by permission from Elsevier. (D) Schematic diagram of ΔG for the three nitrogen-doped configurations in the first electron reduction process and plot of specific activity versus cycling number for graphite N. Reproduced from Wang *et al.*^[109] by permission from ACS. (E) ORR-catalyzed cycle for the conversion of graphitic N to pyridine N. Reproduced from Kim *et al.*^[111] by permission from RSC.

[Figure 5C]. Meng *et al.* prepared carbon hollow skeletons with a high concentration of N doping and disclosed that the ORR active centers were pyrrole N and PNG based on experimental analysis and theoretical calculations^[108]. Some other scholars believe that graphite N is the active site of the catalyst. Wang *et al.* discuss these three doping types in a combined DFT calculation and experimental approach^[109]. Experiments have shown that ORR activity decreases with potential cycling, and the degree of decrease correlates with the decrease in the concentration of graphite N in the catalyst. DFT calculations suggested that the Gibbs free energy change of the first electron reduction of O₂ on the carbon atom adjacent to graphite N was lower compared to PNG and pyrrole N [Figure 5D]. The Above results indicate that graphite N is the main active site of ORR catalysts in basic solutions. Liu *et al.* fabricated newly N-doped ordered mesoporous graphite arrays based on the nanocasting technique^[110]. Their comparison of carbon materials formed with various carbon precursors and at various pyrolysis temperatures shows that GNG is an effective active site in ORR^[110]. Therefore, the catalytic contributions of PNG and GNG to ORR need to be further investigated to learn about active sites of carbon-based catalysts. Kim *et al.* discovered that GNG can turn into PNG through ring opening of cyclic C-N bonds, and this new N-doped active site that interconverts from GNG to PNG can be a new idea to understand the above controversy [Figure 5E]^[111]. PNG and graphite N were investigated for their ORR activity by Wang *et al.* employing DFT^[112]. The O₂ protonation free energy change on GNG is lower than that of PNG, and the results demonstrate that GNG has superior ORR catalytic performance for the same electron transport capacity. In addition, they combined the amounts of N doping, electrical conductivity, and thermodynamic ORR free energy together to evaluate the ORR activity. It was shown that GNG exhibited higher ORR activity when the N-doping concentration was less than 2.8%; this is because ORR activity was determined by the protonation energy change of O₂. The PNG exhibits higher activity when the N-doping concentration is greater than 2.8%, which is derived from the fact that the ORR performance is dictated by the conductivity. Moreover, because of the low stability of five-membered heterocycles, pyrrole N is not commonly found in carbon materials and, therefore, has received less attention. However, pyrrole N is considered to be a potential active site. Li *et al.* proposed that the N-doped ordered mesoporous carbon in pyrrole N has higher ORR activity than

in graphite N^[113]. Although the instability of pyrrole N limits its development, pyrrole N can synergize with other active sites to promote the intrinsic ORR activity of catalysts^[114]. The combination of various nitrogen sites may produce excellent synergistic effects to enhance ORR activity, which opens new directions for design of N-doped electrocatalysts.

In addition to N-doped type active sites, defect-rich carbon can also constitute defective sites for highly active catalytic ORRs, such as zigzag and armchair edges, vacancies, voids, and Stone-Wales defects. Liu *et al.* reported the Plasma-etched carbon cloth (P-CC) with abundant ORR active sites^[115]. They demonstrated through DFT that P-CC had a low overpotential equivalent to that of PGM catalysts, which was attributed to a high number of defective sites. Shen *et al.* deposited air-saturated droplets on the surface of the highly oriented pyrolytic graphite (HOPG) to investigate the ORR activity at different locations^[116]. Electrochemical studies indicated that the edge was more reactive than the substrate surface. They also confirmed by DFT computations that a larger charge density on edge carbon defective sites was essential for higher catalytic activity. Tao *et al.* reported edge-rich graphene as a high-performance ORR catalyst^[117]. The research revealed that edge carbon was important in catalyzing ORR without any other dopant interference, specifying the significance of the defective sites. Xue *et al.* prepared graphene nanoribbons (GNR) with zigzag edges, which were promising electrocatalysts for PEMFCs^[118]. The ORR performance and stability of zigzag carbon are better than that of most non-metallic carbon-based catalysts. They calculated the free energy of the ORR procedure on five types of carbon atoms by the DFT method to identify the active site on GNR [Figure 6]. The results demonstrate that zigzag carbon atoms (a) exhibited better catalytic performance for ORR than basal plane carbon (b), oxidized zigzag carbon (c), armchair edge carbon (d), and carbon atoms near a void (e). This work provided evidence of the great role of defective graphitic carbon in PEMFCs. Furthermore, the catalyst ORR activity can be remarkably enhanced by constructing synergistic coupling sites with N dopants and inherent carbon defects (N/DC)^[115]. Ye *et al.* synthesized a metal-free carbon material enriched with N/DC coupling sites^[119]. It was suggested that the N/DC coupling sites enhanced the electron-donating ability and binding energy of intermediates and boosted the ORR intrinsic activity. Zhang *et al.* proposed the fabrication of edge-rich nitrogen and graphite-like N-doped carbon nanoflakes (NCFs) by the N modification strategy and tandem catalytic graphitization^[120]. This study confirmed that the high ORR performance originated from the electronic synergy of the pyridine-N/graphite N dipole. The results indicate that armchair edge peak carbon atoms are identified as the best active sites for adsorption of oxygen-containing species.

To conclude, the best active site for N doping has been controversial, mainly between PNG and graphite N. The cross-conversion between PNG and graphite N in the catalytic ORR cycle is further suggested to resolve this dispute. However, most scholars believe that PNG has the strongest catalytic ORR effect. Since PNG has lone pair electrons, it enhances the adsorption of reactants and lowers the charge repulsion barrier, thus facilitating the electrocatalytic activity of ORR. Furthermore, the synergy of multiple active sites can greatly strengthen ORR performance, yet the investigation of its essential mechanism is still in its initial period, and the in-depth study of regulatory mechanisms is needed to direct the design of the frontier electrocatalysts. Numerous studies have confirmed that defective sites in carbon matrices are critical in promoting ORR activity. Nevertheless, defects are unstable factors, and how to obtain abundant defective sites with high stability and ORR catalytic capacity in carbon materials will require more in-depth studies in the future.

Non-metallic other heteroatom-doped carbon-based catalysts

Apart from N atoms, the introduction of other heteroatoms, such as B, P, and S, in carbon-based materials for sp² carbon modification might enhance ORR electrocatalytic activity of materials. Kou *et al.* successfully

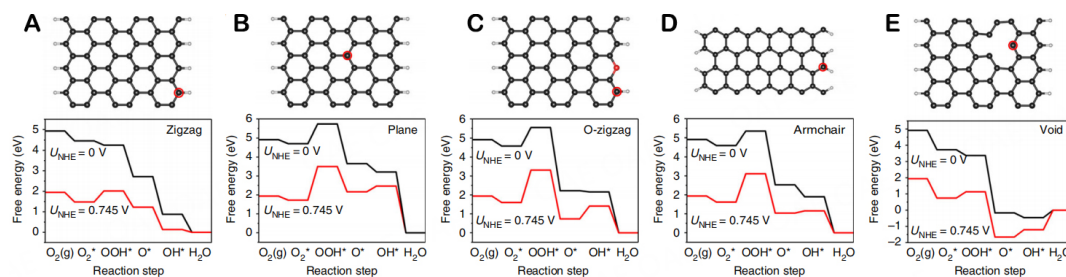


Figure 6. Models of carbon atoms with different edge structures (top) and the corresponding free energy plots (bottom). Reproduced from Xue *et al.*^[118] by permission from Springer Nature.

fabricated BCICNTs by chemically shearing two-dimensional boron carbide^[121]. Theoretical calculations indicate that B is the electron acceptor and Cl is the electron donor in carbon nanotubes. The synergy between these elements aims to increase ORR performance of catalysts, exhibiting higher starting potentials. Zhao *et al.* prepared two types of CNTs co-doped with bonded or separated B and N^[122]. Theoretical calculations showed that B atoms are active sites for O₂ adsorption. For the bonded case, neutralization between the electrons of N and the vacant orbitals of B occurs, resulting in the bonded CNT that is unfavorable for O₂ adsorption. In contrast, the isolated CNT exhibited excellent ORR performance. The results fully demonstrated that heteroatoms had a critical role in the regulation of catalyst ORR activity and provided novel ideas for the exploration of advanced multi-doped carbon-based catalysts. Jiang *et al.* fabricated the porous carbon network with P and N co-doping by pyrolyzing a mixture of supramolecular gels and carbon quantum dots^[123]. The ORR performance of the proposed catalyst was equivalent to and even more stable than commercial Pt/C. Gao *et al.* used N-doped carbon submicron tubes (N-CST) as materials to investigate the principle of designing ORR double-doped catalysts^[124]. It was found that P doping yielded higher ORR catalytic activity than B doping and S doping with lower doping content. They employed DFT calculations to elucidate that the edge C around the oxidized P site located near the graphite N atom was the main active site. Zan *et al.* reported 3D layered micro/mesoporous carbon ternarily doped with S, N, and P, which possesses abundant surface ORR active sites^[125]. X-ray absorption near-edge spectroscopy indicated that S doping increased the type of active sites of catalysts, and the reduced form of S dopant was more critical in ORR electrocatalytic processes.

To sum up, heteroatoms are crucial in non-metallic carbon-based electrocatalysts. The introduction of heteroatoms not only modifies carbon structures (e.g., easy mass transfer voids and highly active defects) to enhance electrocatalytic activity but also modifies the charge and spin density by introducing multiple dopants to modulate the inherent activity of active sites.

Table 1 shows the comparison of ORR performance of PGM-free carbon-based catalysts mentioned previously, and these works have contributed significantly to the classification of active sites in ORR. Furthermore, with the rapid development of technology, active sites of carbon-based catalysts can be directly identified via modern physical assays, such as XPS, XAS, XRD, TEM, atomic force microscopy (AFM), scanning electrochemical microscopy (SECM), electrical transport spectroscopy (ETS), electron energy-loss spectroscopy (EELS), Raman spectroscopy, Mössbauer spectroscopy, nuclear magnetic resonance spectroscopy (NMR), small-angle X-ray scattering (SAXS), TOF-SIMS, inductively coupled plasma-mass spectrometry (ICP-MS), and nuclear resonance vibrational spectroscopy (NRVS). *In situ* testing to capture intermediates provides a clearer view of active site variation during ORR, enabling us to better analyze the composition, characteristics, and mechanisms of these active sites.

Table 1. Comparison of ORR performance of PGM-free carbon-based catalysts

Heteroatom	Catalyst	Morphology	Electrolyte	E_{onset} (V)	$E_{1/2}$ (V)	Ref.
Mn, N	Mn-PANI/C-Mela	Graphene-like	0.1 M HClO ₄	0.78	0.56	[57]
			0.1 M KOH	0.92	0.82	
Fe, N	Fe-PANI/C-Mela	Graphene-like	0.1 M HClO ₄	0.91	0.76	[57]
			0.1 M KOH	1.01	0.88	
Co, N	Co-PANI/C-Mela	Disordered carbon	0.1 M HClO ₄	0.86	0.72	[57]
			0.1 M KOH	0.97	0.87	
Ni, N	Ni-PANI/C-Mela	Nanosheet	0.1 M HClO ₄	0.70	0.48	[57]
			0.1 M KOH	0.89	0.81	
Cu, N	Cu-PANI/C-Mela	Graphene-like	0.1 M HClO ₄	0.80	0.56	[57]
			0.1 M KOH	0.93	0.84	
Fe, N	Fe-N ₂ /C	N/A	0.1 M HClO ₄	0.80	0.67	[59]
			0.1 M NaOH	0.95	0.84	
Fe, N, S	Fe/SNC	Rod-like framework	0.5 M H ₂ SO ₄	N/A	0.77	[61]
Fe, N	ZIF-NC-0.5Fe-700	Dodecahedral shape	0.5 M H ₂ SO ₄	N/A	0.84	[62]
Fe, N	FeNC-1000	Dodecahedral shape	0.5 M H ₂ SO ₄	0.89	0.80	[63]
			0.1 M KOH	0.99	0.90	
Fe, N	Fe-N-C-900	Hierarchically porous	0.1 M KOH	0.99	0.93	[64]
Fe, N	FePc/AP-GA	Nanosheet	0.1 M KOH	0.97	0.87	[67]
Fe, N, S	PpPD-Fe-C	Nanosheet	0.5 M H ₂ SO ₄	0.83	0.72	[68]
Fe, N	(CM+PANI)-Fe-C	Hierarchically porous	0.5 M H ₂ SO ₄	N/A	0.80	[70]
Fe, N	FeN ₂ /NOMC-3	Rod-like framework	0.1 M KOH	1.05	0.86	[71]
Fe, N	O _x BP-Fe	N/A	0.1 M KOH	0.99	N/A	[72]
Fe, N	Fe-N-C	Dodecahedral shape	0.1 M HClO ₄	N/A	0.77	[76]
Fe, N	Fe-AC-CVD	Dodecahedral shape	0.5 M H ₂ SO ₄	N/A	0.85	[77]
Fe, N	SA-Fe/NG	Graphene-like	0.1 M HClO ₄	0.90	0.80	[78]
Fe, N	Fe-N ₂ /C-60	N/A	0.1 M HClO ₄	N/A	0.80	[79]
Fe, N	FeN _x /GM	Graphene-like	0.5 M H ₂ SO ₄	N/A	0.80	[81]
N, S	NSCA-700-1000	Hierarchically porous	0.1 M HClO ₄	0.89	0.76	[84]
			0.5 M H ₂ SO ₄	0.89	0.76	
N	NG-900	Nanosheet	0.1 M KOH	-0.03 vs. Ag/AgCl	N/A	[87]
Fe, N	Fe3-NG	Nanosheet	0.1 M KOH	1.03	0.84	[90]
Fe, N	Fe/Fe ₃ O ₄ @N-G	Nanosheet	0.1 M KOH	N/A	0.85	[91]
Fe, N	Fe-CZIF-800-10	Nanosheet	0.1 M KOH	0.98	0.83	[92]
Fe, N, S	FeNC-S-Fe _x C/Fe	Core-shell fibers	0.1 M HClO ₄	1.05	0.873	[97]
Fe, N	GL-Fe/Fe ₅ C ₂ /NG-800	Nanosheet	0.1 M KOH	0.80	0.60	[98]
Fe, N	Fe-CNSs-N	Nanosphere	0.1 M KOH	0.95	0.84	[99]
Fe, N	Fe ₃ O ₄ @NC/NHPC	Hierarchically porous	0.5 M H ₂ SO ₄	0.90	0.80	[101]
N	NA-CCNT/GC	Nanotube	0.1 M KOH	-0.22 vs. Ag/AgCl	-0.10 vs. Ag/AgCl	[102]
N	Sp-N-doped FLGDY	Nanosheet	0.1 M KOH	N/A	0.87	[103]
N	BPN-100	N/A	0.1 M KOH	N/A	-0.179 vs. SCE	[105]
N	CNT _{PMVI}	Nanotube	0.5 M H ₂ SO ₄	0.46 vs. Ag/AgCl	N/A	[106]
N	NC-600	Flower-like	0.1 M NaOH	N/A	0.30 vs. SCE	[107]
N	NC-800	Hollow framework	0.1 M KOH	N/A	0.85	[108]
N	PDI-900/GC	Rod-like framework	0.1 M KOH	-0.13 vs. Ag/AgCl	N/A	[110]

N	N-OMC ₂	Ordered mesoporous	1.0 M HClO ₄	0.56 vs. Ag/AgCl	N/A	[113]
N	PANI_O ₂ -1000_N ₂ -1200	N/A	0.1 M KOH	0.90	N/A	[114]
N	P-CC	Nanosheet	0.1 M KOH	0.76	N/A	[115]
N	P-G	Nanosheet	0.1 M KOH	0.91	0.74	[117]
N	N-GNR@CNT	Nanotube	0.1 M KOH	0.99	0.84	[118]
N, Br	N/C-Br _{0.3}	Nanosheet	0.1 M HClO ₄	N/A	0.75	[119]
			0.1 M KOH	N/A	0.90	
N	NCF	Nanosheet	0.1 M KOH	1.00	0.85	[120]
B, Cl	BCICNTs	Nanotube	0.1 M KOH	0.94	0.84	[121]
N, P	NPCN-900	Porous networks	0.1 M KOH	0.92	0.78	[123]
			0.5 M H ₂ SO ₄	0.74	0.51	
N, P	N,P-CST	Nanotube	0.1 M KOH	N/A	0.81	[124]
N, P, S	S,N,P-HPC-1	Hierarchically porous	0.1 M KOH	N/A	0.88	[125]

CATALYTIC ACTIVITY ENHANCEMENT STRATEGY

The exploitation of high-performance ORR catalysts is essential to enhance energy conversion efficiencies of catalytic reactions and decrease energy consumption costs, and high performance often derives from excellent catalytic activity. This chapter discusses four up-to-date strategies to boost the electrocatalyst ORR activity. Firstly, the most easily understood strategy is to enhance the intrinsic performance of each active site. Secondly, rapid reactant entry into the catalyst layer and full utilization of each active site can significantly boost active site utilization and catalytic activity, which can be explained by the increased specific surface area and porosity for mass transport and active site exposure. Next, extensive research has confirmed the beneficial impact of defects on the improvement of electrocatalytic performance; thus, enrichment of defects in carbon structures is one of the effective approaches. In addition, highly conductive carbon materials facilitate the charge transfer capability, resulting in excellent electrocatalytic activity; thus, charge transfer is also a promising strategy to enhance catalyst activity.

Boosting intrinsic activity

The essence of ORR is the procedure by which the electrocatalyst adsorbs reactants to specific active sites to create intermediates, i.e., electronic interactions between reactants and active sites. The root problem of PGM-free carbon-based electrocatalysts is their poor intrinsic activity, which is nearly an order of magnitude below that of PGM electrocatalysts. Adjustment of the electronic structure in favor of adjusting the adsorption capacity, energy band structure, and electronic states; thus, optimizing the intrinsic activity is an efficient approach to addressing this fundamental issue^[126].

Yang *et al.* revealed that the charge, ligand effect, and spin density of carbon active sites jointly determine their intrinsic activity and ORR mechanism^[127]. They referred to this finding as the triple effect. The “triple effect” affects the binding energy of *OOH, and the ability of each effect to regulate the binding energy of *OOH follows the following order: high spin effect > ligand effect > low spin effect > positive charge effect > negative charge effect [Figure 7A]. The results demonstrated that the intrinsic ORR electrocatalytic activity can be further improved by the triple effect that can effectively modulate the doping atoms.

Doping engineering is considered to be an efficient way to enhance intrinsic activity of active sites and the rate of ORR reaction. Pei *et al.* produced graded porous N, O, and S co-doped carbon materials with SiO₂ as a template^[128]. The reported carbon materials had great ORR performance, exhibiting half-wave potentials of 0.85 V in basic solutions. Guo *et al.* reported that the S-doped Mn-N-C electrocatalyst was prepared by an efficient adsorption pyrolysis method^[129]. The introduction of S dopants largely enhanced the intrinsic

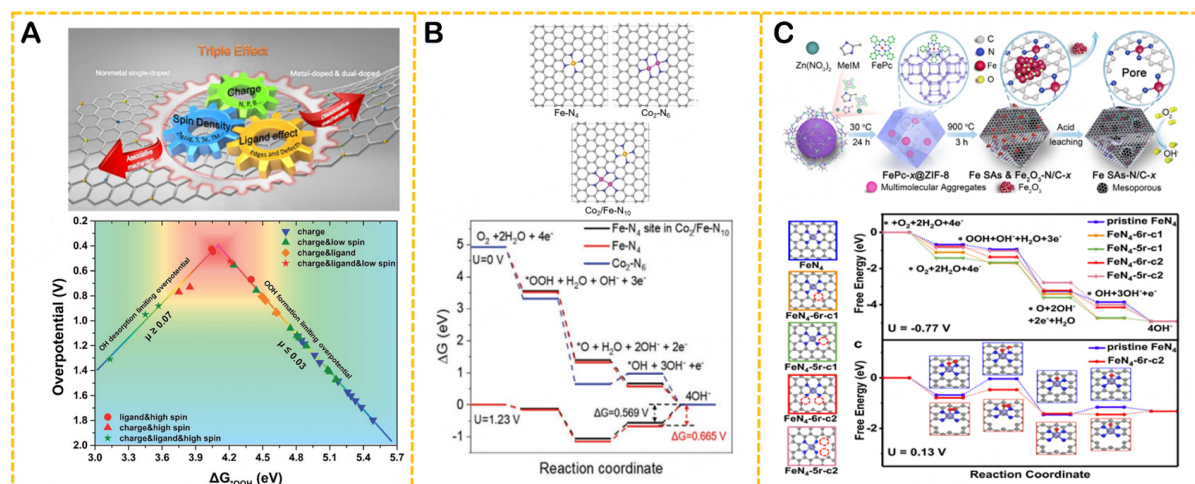


Figure 7. (A) Relationship between ΔG at the carbon active site and ORR overpotential (triple effect). Reproduced from Yang *et al.*^[127] by permission from RSC. (B) Illustration of atomic configurations of each site and free energy plots for each site at U = 0 V and U = 1.23 V. Reproduced from Wang *et al.*^[131] by permission from Wiley-VCH. (C) Schematic illustration of synthesis and free energy plot at U = -0.77 V and U = 0.13 V. Reproduced from Jiang *et al.*^[136] by permission from ACS.

activity of MnN₄. Theoretical computation indicated that the increase in intrinsic ORR activity results mainly from the repulsive interaction on the part of oxygen-containing intermediate and adjacent S dopant, which weakens the intermediate adsorption and promotes the desorption process. Liu *et al.* fabricated modified N-doped carbon with single-atomic Fe and Cu coexistence by hydrothermal synthesis of Fe and Cu co-doped ZIF-8 after pyrolysis in a N₂ atmosphere^[130]. The results showed that the introduction of CuN₄ sites is crucial for enhancing the electronic structure of FeN₄ and speeding up the desorption of oxygen-containing species. Wang *et al.* developed the introduction of Co₂N₆ sites into Fe-N-C electrocatalysts, and the Co₂N₆ sites increased the number of Fe-centered antibonding orbitals on the FeN₄ sites, lowering the energetic barrier of the speed limit step and enhancing ORR intrinsic activity of active sites [Figure 7B]^[131]. Yin *et al.* showed by theoretical calculations that doping P in edge FeN₄ rearranged the surrounding charges and reduced the band gap center of FeN₄, causing an increased tendency for a direct ORR four-electron pathway, which displayed excellent intrinsic ORR performance compared to edge FeN₄ without P^[132].

Spin electrocatalysis is an important topic under development, and it has been shown that doping S in carbon materials can trigger higher spin densities, which are considered to be more favorable sources of activity. In-depth understanding and design of the spintronic oxygen electrocatalysis are crucial for ORR electrocatalyst development^[133]. Yang *et al.* rationalized design of bimetallic atom-dispersed M-N-C electrocatalysts, revealing that 3d orbitals in transition metals were significant pathways to optimize the intrinsic activity of active centers^[134]. Experiments and theoretical calculations together showed that the adjacent atom-dispersed Mn-N could activate the Fe(III) sites by electron modulation and spin state transition, resulting in excellent ORR performance and stability of this catalyst in both acidic and basic solutions. The results indicated that regulating metal species with moderate spins was an effective way to enhance the ORR performance, yet how easily the spin state can be controlled still limits the development of this approach. Li *et al.* investigated covalent-organic-polymers-based paradigm electrocatalysts and designed a series of FeN₄ sites with a clear local coordination environment by the pyrolysis-free approach^[135]. The results revealed that the Fe atoms around the electron-absorbing side chains carried more positive charges under the charge modulation driven by the dz² orbital, thus forming a high-valence FeN₄ structure, and the performance-enhancing high intrinsic activity ORR catalysts were obtained by optimizing the center of weight of the 3dz² orbital by about one order of magnitude.

The local coordination environment of central atomic sites may dictate the geometric/electronic structure of carbon-based electrocatalyst active centers. Therefore, modulating the coordination environment is also an efficient method to optimize the catalyst ORR activity. Jiang *et al.* introduced the metal precursor FePc with a size larger than the lumen of ZIF-8 into the main framework, which disrupted the domain-limiting effect of the pre-existing micropores, facilitating the generation of edge FeN₄ active sites, lowering the ORR potential barrier, and improving the intrinsic activity [Figure 7C]^[136]. Gong *et al.* designed the coordination environment of active centers at the atomic scale to obtain high intrinsic activity of FeN₄, which was about 10-fold higher than the normal FeN₄ sites^[137]. They introduced axially bonded O into the Fe sites, and the O-containing ligand served as an electronic structure modulator, which weakened binding strength of Fe to oxygen-containing species, leading to a significant enhancement of ORR performance. Shah *et al.* reported double-doped P, N carbon frameworks with high ORR activity single zinc atom doping by modulating the surrounding coordination environment of active sites^[138]. Charge reallocation caused via multi-heteroatom doping decreased ORR reduction potential barriers, thereby increasing the intrinsic activity of active sites.

Increasing active site density

Based on the Butler-Volmer formula, the $E_{1/2}$ value is directly associated with the active site quantity, which is one of the features of ORR activity. Increasing active site density can increase the contact interface between active sites and reactants, allowing reactants to fully interact with active sites, which is essential for enhancing the carbon-based catalyst activity. The number of active sites is directly associated with the specific surface area of carbon-based materials and pore structures of carbon skeletons.

Since metal migration and the aggregation and agglomeration of organic precursors often occur during pyrolysis, the quantity of accessible active sites tends to decrease with surface area reduction, which is not favorable for catalytic activity enhancement. The concept of “single-atom catalysis (SAC)” has been proposed by some scholars to decrease the size of transition metal carbon-based catalysts to the atomic level^[139]. Since the metal utilization rate is up to 100%, SAC greatly improves the specific surface area and specific activity of catalysts and enhances ORR performance. Yin *et al.* realized stable atomic dispersion of Co monoatoms on N-doped carbon materials^[140]. The strategy is on the basis of a pyrolysis process of the bimetallic MOF, where the carbonization of the organic linker reduces Co, and Zn is optionally evaporated at high temperatures beyond 800 °C [Figure 8A]. Active site density could be significantly increased to prepare the high SAC for ORR performance by manipulating the Zn/Co ratio. The prepared CoN_x active sites displayed high ORR performance with a positive half-wave potential of 0.881 V. Li *et al.* used the spatially constrained approach to encapsulate molecular cages in ZIF materials as metal precursors^[141]. Atomically dispersed N-ligated Mn catalysts on graphitic carbon with high active site density were obtained, and the Mn-N-C catalysts displayed a positive half-wave potential of 0.80 V. Xin *et al.* developed Fe-N-C single-atom electrocatalysts with a graded porous nanosheet morphology with the specific surface area of 2,237 m²·g⁻¹ via molten salt-mediated pyrolysis strategy [Figure 8B]^[142]. They utilized intense polarity and salt-template effects to regulate the electronic structure and morphology of electrocatalysts, whose ORR activity was controlled by the axially bound Cl in the FeN₄Cl site. The Fe-N-C catalyst showed exceptional ORR performance in the basic medium, which was greater than the benchmark Pt/C. Similarly, Li *et al.* proposed a single-atom cobalt electrocatalyst with enhanced mesoporosity, which favors mass transfer and increases the active site accessibility^[143]. It was shown that Co SAs/NC showed significant mass transfer and electron transfer, exhibiting strong ORR performance. In addition, increasing the specific surface area is also commonly applied to enhance the active site density of inorganic non-metallic carbon-based catalysts. Ding *et al.* developed the “Shape Fixing via Salt Recrystallization” method^[144]. They immobilized and completely sealed the FeCl₃-loaded 3D-PANI within NaCl by recrystallization of NaCl solution to obtain NaCl-sealed PANI [Figure 8C]^[144]. Subsequently, the CPANI-Fe-NaCl catalyst was obtained by carbonization at 900 °C, and its specific surface area increased from the initial 30.7 m²·g⁻¹ to 265.7 m²·g⁻¹.

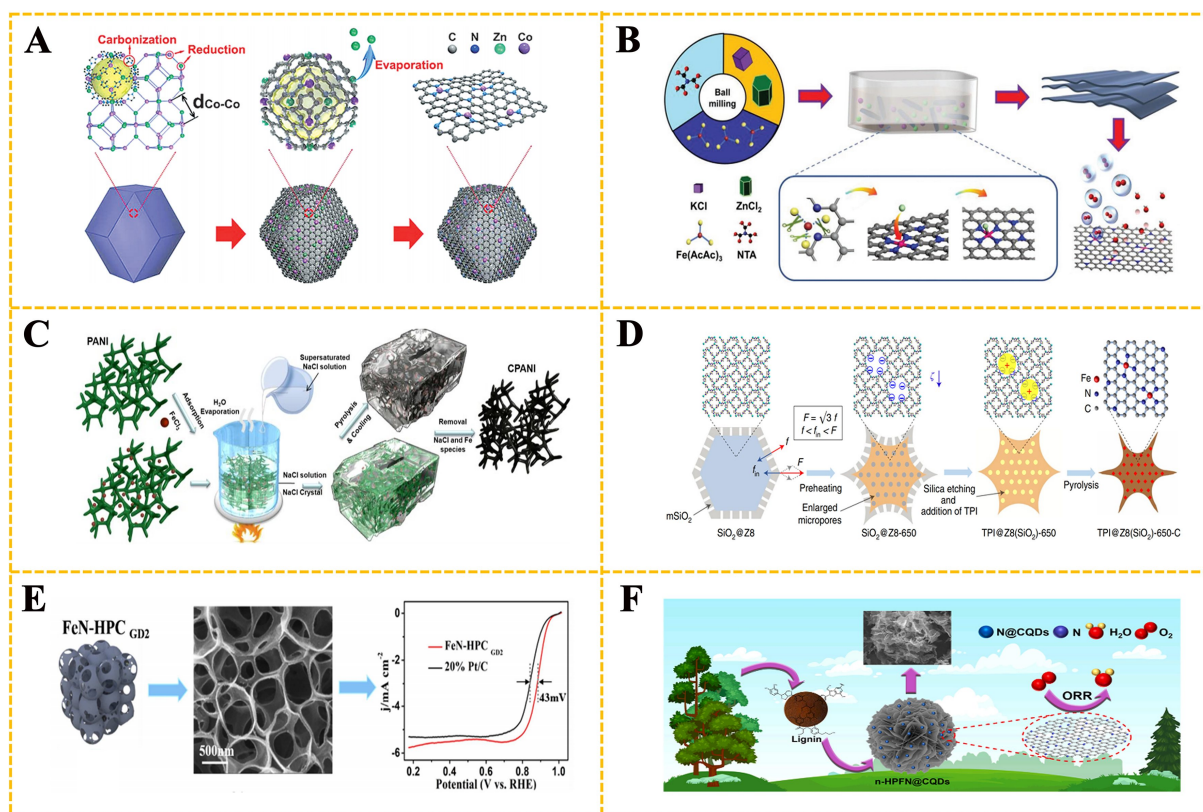


Figure 8. (A) The preparation method of Co SAs/N-C. Reproduced from Yin *et al.*^[140] by permission from Wiley-VCH. (B) Schematic diagram of the molten-salts mediated pyrolysis method of Fe-N/C-SAC. Reproduced from Xin *et al.*^[142] by permission from Wiley-VCH. (C) Schematic diagram of the "Shape Fixing via Salt Recrystallization" strategy. Reproduced from Ding *et al.*^[144] by permission from ACS. (D) Synthesis of TPI@Z8(SiO₂)-650-C. Reproduced from Wan *et al.*^[145] by permission from the Springer Nature. (E) Morphology and electrochemical characterization of FeN-HPC. Reproduced from Chen *et al.*^[147] by permission from Elsevier. (F) The formation of n-HPFN@CQDs. Reproduced from Ma *et al.*^[150] by permission from Elsevier.

Large surfaces facilitated the active site exposition to increase the availability, and the catalyst had an output power of as high as 600 mW·cm⁻² in PEMFCs.

Ideal porosity, such as carbon skeletons with graded porous structures (especially with mesopores), facilitates the exposition of more active sites and is a premise for maximizing the active site properties. At the same time, high porosity promotes mass transfer to strengthen the interplay between active sites, electrons, and reactants prior to each other. For transition metal carbon-based catalysts, MN₄ is mostly recognized as the active site of catalysts, and research revealed that a certain amount of MN₄ is found in the micropores in carbon materials. However, it is difficult for protons and reactants to enter the micropores with tiny pore sizes (no more than 2 nm) due to the mass transfer limitation, which results in undesirable electrocatalytic activity^[62]. Therefore, the rational design of high porosity materials is essential for ORR performance enhancement. Increasing the mesoporosity of carbon materials can provide effective mass transfer channels for MN_x active sites within the dense 3D carbon backbone to increase the active site accessibility and ORR activity. Wan *et al.* developed a concave Fe-N-C single-atom catalyst with high surface area and mesoporosity [Figure 8D]^[145]. It was shown that the high active site density of catalysts stems from the exposure of inaccessible FeN₄ sites and enhanced mass transport in catalyst layers. They demonstrate through quantitative structure-property correlation that active site density was the main determinant of catalyst current density in fuel cells. Qiao *et al.* prepared porous carbon materials possessing

atomically dispersed sites by pyrolysis of hierarchically ordered porous materials with Fe-doped single crystal ZIF-8^[146]. In PEMFCs, FeN₄/C without macro-mesoporous showed low ORR catalytic efficiency, and the study demonstrated that the prepared hierarchically ordered porous carbon had a higher active site density and stronger mass transfer capability. Meanwhile, they also found that optimizing the Fe doping level could maximize the catalyst ORR activity. Purposeful design of thin nanosheets with hierarchical porous carbon structures can add area to the reaction interface and improve the exposure of active sites. Chen *et al.* used NaCl-assisted pyrolysis to fabricate FeN-HPC ultrathin carbon nanosheets [Figure 8E]^[147]. FeN-HPC has a hierarchical structure with high surface area and macro-meso-micro pores and displays excellent ORR catalytic performance, even surpassing commercial Pt/C, owing to its loading of a remarkably high percentage (93.7%) of pyridine N and graphite N. Similarly, Zhang *et al.* developed anchored in honeycomb N-doped carbon materials with MN₄ active sites displaying superior ORR electrocatalytic activity through a two-step calcination using NaCl as a template^[148]. Furthermore, for non-metallic carbon-based materials, the appropriate porosity facilitates increased density of active sites and electrolyte penetration and reactant transport, resulting in high ORR activity. Nanoporous carbon prepared using biomass and waste feedstock plays a huge role in ORR electrocatalysis and sustainable energy, improving performance while reducing and avoiding environmental pollution^[149]. Ma *et al.* deposited aminated lignin-based carbon quantum dots (n-CQDs) *in situ* on the prepared hierarchical porous N-doped 3D nanosheets of lignin to obtain the N-doped hierarchical porous flower-like carbon nanosheets decorated with n-CQDs (n-HPFN@CQDs) [Figure 8F]^[150]. Benefiting from the synergistic effect of n-CQDs and porous carbon materials, the hierarchical porous structure of n-HPFN@CQDs exhibits both a high electrochemically active surface area and exposes numerous active sites with reduced conduction/mass transfer resistance, thus exhibiting superior electrocatalytic activity. Liu *et al.* fabricated 3D hierarchical porous carbon nanosheets using biomass water lettuce as precursors^[151]. They indicated by electrochemical studies that this catalyst not only had a high ORR active site density but also exhibited great ORR intrinsic performance at each active site in most electrolytes. Jalalah *et al.* synthesized N-doped graphitized carbon-based materials (BV-800) using green common bamboo leaves as precursors and anhydrous NH₄NO₃ as nitrogen sources by chemical synthesis and subsequent heat treatment^[152]. The excellent ORR performance was derived from the high porosity, specific surface area, and nitrogen content of BV-800, which facilitated the exposure of active sites and increased active site density. In addition, BV-800 has good four-electron reaction selectivity with an electron transfer number of 3.95^[152].

Enriching defects

The second law of thermodynamics shows that carbon-based catalyst materials always contain defects or disordered structures on their surfaces or edges^[153]. Defects in carbon materials can not only modulate spin density and charge state of the electronic structure to distort the carbon structure but also lead to strong adsorption of intermediates by the charge polarization of carbon atoms to enhance the ORR performance^[154]. To date, there has been a large amount of research showing that defect engineering can contribute to adding a variety of active sites and maximizing the active site density. Liu *et al.* found that highly graphitized carbon structures have difficulty accommodating sufficient active site density due to their lack of abundant defects^[77]. They modulated the carbon structure and coordination environment by high-temperature NH₄Cl heat treatment of ZIF-8 precursors, which produced abundant defects to improve active site density. Qiao *et al.* prepared N-doped carbon materials via pyrolysis of chitosan with molten salt and demonstrated that the high active site density of catalysts was explained by the abundant defect content and large specific surface area in catalysts; thus, catalysts exhibited excellent ORR catalytic activity^[155]. Cheng *et al.* explored the synergistic interaction between MN₄ and defective sites^[156]. They synthesized M-N-C electrocatalysts with two types of active centers (MN₄ and carbon defects) in one step by wet chemistry. It was found that the introduction of defects not only improved active site density but also changed the spin state of Fe, which synergistically strengthened the ORR performance. The HOPG was investigated in detail

by Jia *et al.*^[157]. It was experimentally and theoretically demonstrated that the pentagonal edge defects resulting from the removal of Pr-N atoms from the N-doped six-carbon ring were the major active sites with better activity than Pr-N in the N-doped HOPG. The results suggested that purposeful defect engineering of carbon materials might lead to increased ORR activity and quantity of active sites, providing ideas for the exploitation of high-performance catalysts. Likewise, Li *et al.* adopted defect engineering to treat hierarchical porous carbon aerogels and discovered that high ORR performance of the S-C coordination structure was owing to the low-activation energy resulting from introduction of abundant defects via S doping^[84]. In addition, they found that introducing graphite N atoms into S-C defects in the catalyst produced higher ORR activity. Subsequently, the N-S-C defect structure in the carbon aerogel was the newly generated ORR active site. Theoretical computations suggested that the synergy of edge pentagonal defects and N, S atoms was essential to boost catalyst performance and that adding the amounts of active sites was an attractive approach to enhance the catalyst ORR activity.

Charge transport

A high conductivity electrocatalyst implies a faster charge transfer capability, which benefits the adsorption/desorption of reactants, intermediate species, and products, promoting an orderly and stable reaction. The catalyst activity is often closely associated with the adsorption/desorption of reactants, intermediate species, and products; thus, increasing the charge transport capacity of catalyst materials is essential to enhance catalyst activity. In addition, for ORR, undesired two-electron reaction pathways can also be decreased by improving the conductivity of catalysts. The electrical conductivity of carbon-based catalysts is intimately associated with the degree of graphitization. And a high graphitization degree of carbon material needs to be achieved by the pyrolysis process. Generally, the annealing temperature of carbon-based electrocatalysts and the degree of carbon graphitization and electrical conductivity are positively correlated. It was revealed that ORR performance was positively correlated with electrical conductivity over the entire potential range by testing ORR performance of N-doped carbon nanotubes prepared at various temperatures^[158]. Moreover, excessive annealing temperatures may affect the catalyst ORR activity by causing structural damage to the carbon material and active site. Therefore, balancing the relationship between the two to obtain optimal ORR activity is an important approach to optimizing carbon-based electrocatalysts.

PERSPECTIVES AND OUTLOOK

PGM-free carbon-based catalysts are ideal materials for ORR electrocatalysis to replace precious metal catalysts. They perform outstanding activity and durability while reducing cost. Herein, we comprehensively analyzed the ORR mechanisms and the active site classification of transition metal-doped carbon-based catalysts and non-metallic N-doped carbon-based catalysts and elucidated the intrinsic relationship between structures and functions of active sites. Based on this, we propose an exhaustive strategy for the catalyst activity enhancement from the active site perspective. In general, the commitment to develop carbon-based catalysts with high activity and active site density is the key to enhancing ORR performance of catalysts. On the basis of the adjustments to the electronic structure, spin density, and coordination environment, some PGM-free carbon-based catalysts exhibit comparable or even superior ORR performance than commercial Pt/C.

However, electrocatalyst stability is a tremendous challenge for most PGM-free carbon-based catalysts. There are currently four possible degradation mechanisms for PGM-free carbon-based catalysts: oxidation of H₂O₂, protonation of N, demetallation, and microporous flooding. Incomplete oxidation of ORR may generate intermediate products, H₂O₂, which can directly or indirectly destroy the active site structure, while more H₂O₂ may be generated, which will pose a significant threat to the stability of the catalysts. Therefore, avoiding or reducing the generation of H₂O₂ is an obvious approach to enhance the stability of catalysts.

Since N atoms have a lone pair of electrons, they can be attacked by H protons to generate NH. Many carbon-based catalysts possess a significant amount of N, which may be involved in constituting the active site, and N attacked by H protons will lose ORR activity, thus reducing the stability of the catalyst. Demetallation may cause a decrease in the density of active sites and, thus, a decrease in catalytic activity. The metal ions formed by demetallation can catalyze H_2O_2 to produce free radicals that cause carbon oxidation or damage the proton exchange membrane. In addition, carbon oxidation may cause the destruction of the MN_4 active site and thus accelerate demetallation. Flooding of micropores may lead to blocked mass transfer and thus reduce catalyst activity. Furthermore, increasing the graphitization of carbon materials enhances catalyst stability by improving corrosion resistance. However, highly graphitized carbon materials may decrease the amounts of active centers and, thus, catalytic activity. The trade-off of activity and stability is an important issue for the future development of PGM-free carbon-based ORR electrocatalysts.

Numerous strategies have been developed to improve the stability of PGM-free carbon-based ORR catalysts, in general, with the following five points: (i) Reduction or elimination of H_2O_2 and reactive oxygen species (ROS). H_2O_2 and ROS generated by side reactions in ORR pose a significant threat to stability. Improving the four-electron selectivity of the reaction at the atomic level by increasing active sites of carbon-based catalysts is beneficial in reducing and eliminating H_2O_2 and ROS. Moreover, the introduction of Ce-based materials, such as CeO_2 , as H_2O_2 and ROS scavengers in the catalyst is an effective solution for the rapid removal of undesirable by-products; (ii) Reduced demetallation of M- N_x sites. Improved electronic coupling between the active site and the carbon matrix facilitates the resolution of demetallation; (iii) Enhancing the corrosion resistance of carbon-based materials. As carbon is thermodynamically favored to undergo electrochemical corrosion and be oxidized, carbon corrosion is an aspect to be considered in stability. Carbon graphitization and edge conditioning are effective methods of improving the corrosion resistance of carbon-based materials. It is important to note that highly graphitized carbon materials often limit the number of active sites. The trade-off between graphitization and porosity needs to be considered, with graphitization favoring stability and increasing the number of micropores to expose more active sites benefiting activity; and (iv) Reduced microporous flooding. Enhancing the hydrophobicity of catalyst materials and designing hierarchically porous structures to improve mass transfer is beneficial in reducing micropore flooding. To date, many effective strategies have been developed to address the stability of carbon-based catalysts, but there are still vast areas to be explored, such as the mitigation of protonation of N that has rarely been reported.

Moreover, the catalyst performance at the rotating disk electrode (RDE) cannot be equated with the membrane electrode assembly (MEA), which is attributed to the fact that the operating temperature, environment, and equipment of MEA are quite different from RDE, e.g., the activity and stability experiments at 60-80 °C. A large number of catalysts with high ORR activity at the RDE level display poor catalytic performance in MEA. For ORR PGM-free carbon-based catalysts, the difference in performance on RDE and MEA is from the lack of sufficient theories and understanding to guide the design of optimal three-phase interfaces for charge and mass transport^[159]. Firstly, as the electrodes in MEA are typically porous thick electrodes containing ionomers, this greatly limits the transport of reactants (O_2 and protons) and hence the accessibility of active sites for PGM-free carbon-based catalysts, resulting in a situation where catalyst ORR activity is not fully revealed. Therefore, optimization of the electrode structure, i.e., the specific surface area and porosity of PGM-free carbon-based catalysts, is essential to enhance MEA performance. An effective strategy is a trade-off between micropores, mesopores, and macropores, with micropores often considered to be the host site for active sites and mesopores and macropores being the key to mass transport of reactants. Secondly, the interface collapse caused by carbon corrosion and changes in ionomer

morphology can affect the performance of MEA. Stabilizing carbon matrixes and ionomers would be an effective way of solving this problem. Finally, severe water flooding of PGM-free carbon-based catalysts will also restrict MEA performance. This is related to factors such as the properties of the catalyst (porosity, surface functionalities, and graphitization degree) and the content of the ionomers. RDE technology has been applied to novel catalysts prepared by large-scale pre-selection, but catalysts need to demonstrate high activity and stability in MEA to broaden their practical applications; thus, incorporating MEA testing in the early stages of catalyst development is expected to decrease this gap.

In conclusion, as the enhanced high ORR activity sites are often more susceptible to complex catalytic environmental factors, PGM-free carbon-based catalysts require trade-offs for activity, durability, power density, and cost, which we believe will soon be resolved in the future to yield tremendous value for PGM-free carbon-based catalysts in PEMFCs.

DECLARATIONS

Authors' contributions

Proposed the topic of this review: Ge J

Wrote the manuscript: Wei K

Reviewed the manuscript: Wang X, Ge J

Contributed to the discussion of the manuscript: Wei K, Wang X, Ge J

Availability of data and materials

Not applicable.

Financial support and sponsorship

The authors would like to thank the National Key R&D Program (2022YFB4004100), National Natural Science Foundation of China (U22A20396, 22209168), Natural Science Foundation of Anhui Province (2208085UD04), and Dalian National Laboratory for Clean Energy (DNL), CAS, the Research Innovation Fund (grant DNL202010) for their financial support.

Conflicts of interest

All authors declared that there are no conflicts of interest.

Ethical approval and consent to participate

Not applicable.

Consent for publication

Not applicable.

Copyright

© The Author(s) 2023.

REFERENCES

1. Thompson ST, Papageorgopoulos D. Platinum group metal-free catalysts boost cost competitiveness of fuel cell vehicles. *Nat Catal* 2019;2:558-61. [DOI](#)
2. Fan Q, Yan S, Wang H. Nanoscale redox reaction unlocking the next-generation low temperature fuel cell. *Energy Mater* 2022;2:200002. [DOI](#)
3. Zhao J, Liu H, Li X. Structure, property, and performance of catalyst layers in proton exchange membrane fuel cells. *Electrochem Energy Rev* 2023;6:13. [DOI](#) [PubMed](#) [PMC](#)
4. Zhang Y, Xiao F, Chen G, Shao M. Fuel cell performance of non-precious metal based electrocatalysts. *J Electrochem* 2020;26:563-

72. DOI
5. Cao S, Sun T, Li J, Li Q, Hou C, Sun Q. The cathode catalysts of hydrogen fuel cell: from laboratory toward practical application. *Nano Res* 2023;16:4365-80. DOI
 6. Hamo ER, Rosen BA. Transition metal carbides as cathode supports for PEM fuel cells. *Nano Res* 2022;15:10218-33. DOI
 7. Nie Y, Li L, Wei Z. Recent advancements in Pt and Pt-free catalysts for oxygen reduction reaction. *Chem Soc Rev* 2015;44:2168-201. DOI
 8. Yang X, Priest C, Hou Y, Wu G. Atomically dispersed dual-metal-site PGM-free electrocatalysts for oxygen reduction reaction: opportunities and challenges. *SusMat* 2022;2:569-90. DOI
 9. Li Y, Chen M, Lu B, Zhang J. Recent advances in exploring highly active & durable pgm-free oxygen reduction catalysts. *J Electrochem* 2023;29:2215002. DOI
 10. Thompson ST, James BD, Huya-kouadio JM, et al. Direct hydrogen fuel cell electric vehicle cost analysis: system and high-volume manufacturing description, validation, and outlook. *J Power Sources* 2018;399:304-13. DOI
 11. Zeng R, Yang Y, Feng X, et al. Nonprecious transition metal nitrides as efficient oxygen reduction electrocatalysts for alkaline fuel cells. *Sci Adv* 2022;8:eabj1584. DOI PubMed PMC
 12. Xia W, Mahmood A, Liang Z, Zou R, Guo S. Earth-abundant nanomaterials for oxygen reduction. *Angew Chem Int Ed* 2016;55:2650-76. DOI PubMed
 13. He Y, Wu G. PGM-free oxygen-reduction catalyst development for proton-exchange membrane fuel cells: challenges, solutions, and promises. *ACC Mater Res* 2022;3:224-36. DOI
 14. Liu J, Ma R, Chu Y, et al. Construction and regulation of a surface protophilic environment to enhance oxygen reduction reaction electrocatalytic activity. *ACS Appl Mater Interfaces* 2020;12:41269-76. DOI
 15. Liu S, Zhang Y, Ge B, et al. Constructing graphitic-nitrogen-bonded pentagons in interlayer-expanded graphene matrix toward carbon-based electrocatalysts for acidic oxygen reduction reaction. *Adv Mater* 2021;33:e2103133. DOI
 16. Chang Y, Chen J, Jia J, et al. The fluorine-doped and defects engineered carbon nanosheets as advanced electrocatalysts for oxygen electroreduction. *Appl Catal B Environ* 2021;284:119721. DOI
 17. Liu K, Fu J, Lin Y, et al. Insights into the activity of single-atom Fe-N-C catalysts for oxygen reduction reaction. *Nat Commun* 2022;13:2075. DOI PubMed PMC
 18. Zhao T, Li Y, Liu J, et al. Highly dispersed L1₂-Pt₃Fe intermetallic particles supported on single atom Fe-N_x-C_y active sites for enhanced activity and durability towards oxygen reduction. *Chin Chem Lett* 2023;34:107824. DOI
 19. Xie S, Jin H, Wang C, et al. A comparison study on single metal atoms (Fe, Co, Ni) within nitrogen-doped graphene for oxygen electrocatalysis and rechargeable Zn-air batteries. *Chin Chem Lett* 2023;34:107681. DOI
 20. Ishihara A, Ohgi Y, Matsuzawa K, Mitsushima S, Ota K. Progress in non-precious metal oxide-based cathode for polymer electrolyte fuel cells. *Electrochim Acta* 2010;55:8005-12. DOI
 21. Wang H, Qiu X, Peng Z, et al. Cobalt-gluconate-derived high-density cobalt sulfides nanocrystals encapsulated within nitrogen and sulfur dual-doped micro/mesoporous carbon spheres for efficient electrocatalysis of oxygen reduction. *J Colloid Interface Sci* 2020;561:829-37. DOI
 22. Yuan H, Kong L, Li T, Zhang Q. A review of transition metal chalcogenide/graphene nanocomposites for energy storage and conversion. *Chin Chem Lett* 2017;28:2180-94. DOI
 23. Lv XW, Xu WS, Tian WW, Wang HY, Yuan ZY. Activity promotion of core and shell in multifunctional core-shell Co₂P@NC electrocatalyst by secondary metal doping for water electrolysis and Zn-air batteries. *Small* 2021;17:e2101856. DOI PubMed
 24. Jasinski R. A new fuel cell cathode catalyst. *Nature* 1964;201:1212-3. DOI
 25. Hu C, Dai L. Carbon-based metal-free catalysts for electrocatalysis beyond the ORR. *Angew Chem Int Ed* 2016;55:11736-58. DOI PubMed
 26. Jiang H, Gu J, Zheng X, et al. Defect-rich and ultrathin N doped carbon nanosheets as advanced trifunctional metal-free electrocatalysts for the ORR, OER and HER. *Energy Environ Sci* 2019;12:322-33. DOI
 27. Wang F, Zhou Y, Lin S, Yang L, Hu Z, Xie D. Axial ligand effect on the stability of Fe-N-C electrocatalysts for acidic oxygen reduction reaction. *Nano Energy* 2020;78:105128. DOI
 28. Wang Q, Lu R, Yang Y, et al. Tailoring the microenvironment in Fe-N-C electrocatalysts for optimal oxygen reduction reaction performance. *Sci Bull* 2022;67:1264-73. DOI
 29. Lu F, Fan K, Cui L, et al. Engineering FeN₄ active sites onto nitrogen-rich carbon with tubular channels for enhanced oxygen reduction reaction performance. *Appl Catal B Environ* 2022;313:121464. DOI
 30. Xu M, Liu J, Ge J, Liu C, Xing W. Research progress of metal-nitrogen-carbon catalysts toward oxygen reduction reaction inm changchun institute of applied chemistry. *J Electrochem* 2020;26:464-73. DOI
 31. Zhang L, Meng Q, Zheng R, et al. Microenvironment regulation of M-N-C single-atom catalysts towards oxygen reduction reaction. *Nano Res* 2023;16:4468-87. DOI
 32. Yang Y, Xiong Y, Zeng R, et al. Operando methods in electrocatalysis. *ACS Catal* 2021;11:1136-78. DOI
 33. Zhao J, Lian J, Zhao Z, Wang X, Zhang J. A review of in-situ techniques for probing active sites and mechanisms of electrocatalytic oxygen reduction reactions. *Nanomicro Lett* 2022;15:19. DOI PubMed PMC
 34. Jia Y, Xiong X, Wang D, et al. Atomically dispersed Fe-N₄ modified with precisely located S for highly efficient oxygen reduction. *Nanomicro Lett* 2020;12:116. DOI PubMed PMC

35. Jiao Y, Zheng Y, Jaroniec M, Qiao SZ. Design of electrocatalysts for oxygen- and hydrogen-involving energy conversion reactions. *Chem Soc Rev* 2015;44:2060-86. [DOI](#) [PubMed](#)
36. Chen G, Sun Y, Chen RR, et al. A discussion on the possible involvement of singlet oxygen in oxygen electrocatalysis. *J Phys Energy* 2021;3:031004. [DOI](#)
37. Borden WT, Hoffmann R, Stuyver T, Chen B. Dioxygen: what makes this triplet diradical kinetically persistent? *J Am Chem Soc* 2017;139:9010-8. [DOI](#) [PubMed](#)
38. Fridovich I. Oxygen: how do we stand it? *Med Princ Pract* 2013;22:131-7. [DOI](#) [PubMed](#) [PMC](#)
39. Biz C, Gracia J, Fianchini M. Review on magnetism in catalysis: from theory to PEMFC applications of 3D metal Pt-based alloys. *Int J Mol Sci* 2022;23:14768. [DOI](#) [PubMed](#) [PMC](#)
40. Biz C, Fianchini M, Gracia J. Strongly correlated electrons in catalysis: focus on quantum exchange. *ACS Catal* 2021;11:14249-61. [DOI](#)
41. Nørskov JK, Rossmeisl J, Logadottir A, et al. Origin of the overpotential for oxygen reduction at a fuel-cell cathode. *J Phys Chem B* 2004;108:17886-92. [DOI](#)
42. Jiang WJ, Gu L, Li L, et al. Understanding the high activity of Fe-N-C electrocatalysts in oxygen reduction: Fe/Fe₃C nanoparticles boost the activity of Fe-N_x. *J Am Chem Soc* 2016;138:3570-8. [DOI](#)
43. Zhao Z, Chen C, Liu Z, et al. Pt-based nanocrystal for electrocatalytic oxygen reduction. *Adv Mater* 2019;31:e1808115. [DOI](#)
44. Prabhakaran V, Wang G, Parrondo J, Ramani V. Contribution of electrocatalyst support to PEM oxidative degradation in an operating PEFC. *J Electrochem Soc* 2016;163:F1611. [DOI](#)
45. Banham D, Kishimoto T, Zhou Y, et al. Critical advancements in achieving high power and stable nonprecious metal catalyst-based MEAs for real-world proton exchange membrane fuel cell applications. *Sci Adv* 2018;4:eaar7180. [DOI](#) [PubMed](#) [PMC](#)
46. Radwan A, Jin H, He D, Mu S. Design engineering, synthesis protocols, and energy applications of MOF-derived electrocatalysts. *Nanomicro Lett* 2021;13:132. [DOI](#) [PubMed](#) [PMC](#)
47. Yao Y, You Y, Zhang G, et al. Highly functional bioinspired Fe/N/C oxygen reduction reaction catalysts: structure-regulating oxygen sorption. *ACS Appl Mater Interfaces* 2016;8:6464-71. [DOI](#)
48. Abild-Pedersen F, Greeley J, Studt F, et al. Scaling properties of adsorption energies for hydrogen-containing molecules on transition-metal surfaces. *Phys Rev Lett* 2007;99:016105. [DOI](#)
49. Biz C, Fianchini M, Gracia J. Catalysis meets spintronics; spin potentials associated with open-shell orbital configurations enhance the activity of Pt₃Co nanostructures for oxygen reduction: a density functional theory study. *ACS Appl Nano Mater* 2020;3:506-15. [DOI](#)
50. Gracia J. Spin dependent interactions catalyse the oxygen electrochemistry. *Phys Chem Chem Phys* 2017;19:20451-6. [DOI](#) [PubMed](#)
51. Zhang L, Cheruvathur A, Biz C, Fianchini M, Gracia J. Ferromagnetic ligand holes in cobalt perovskite electrocatalysts as an essential factor for high activity towards oxygen evolution. *Phys Chem Chem Phys* 2019;21:2977-83. [DOI](#) [PubMed](#)
52. Hong J, Jin C, Yuan J, Zhang Z. Atomic defects in two-dimensional materials: from single-atom spectroscopy to functionalities in opto-/electronics, nanomagnetism, and catalysis. *Adv Mater* 2017;29:1606434. [DOI](#)
53. Wang X, Li Z, Qu Y, et al. Review of metal catalysts for oxygen reduction reaction: from nanoscale engineering to atomic design. *Chem* 2019;5:1486-511. [DOI](#)
54. Martinez U, Komini Babu S, Holby EF, Chung HT, Yin X, Zelenay P. Progress in the development of Fe-based PGM-free electrocatalysts for the oxygen reduction reaction. *Adv Mater* 2019;31:e1806545. [DOI](#) [PubMed](#)
55. Alt H, Binder H, Sandstede G. Mechanism of the electrocatalytic reduction of oxygen on metal chelates. *J Catal* 1973;28:8-19. [DOI](#)
56. Zheng Y, Yang DS, Kweun JM, et al. Rational design of common transition metal-nitrogen-carbon catalysts for oxygen reduction reaction in fuel cells. *Nano Energy* 2016;30:443-9. [DOI](#)
57. Peng H, Liu F, Liu X, et al. Effect of transition metals on the structure and performance of the doped carbon catalysts derived from polyaniline and melamine for ORR application. *ACS Catal* 2014;4:3797-805. [DOI](#)
58. Venegas R, Muñoz-becerra K, Candia-onfray C, Marco JF, Zagal JH, Recio FJ. Experimental reactivity descriptors of M-N-C catalysts for the oxygen reduction reaction. *Electrochim Acta* 2020;332:135340. [DOI](#)
59. Ramaswamy N, Tylus U, Jia Q, Mukerjee S. Activity descriptor identification for oxygen reduction on nonprecious electrocatalysts: linking surface science to coordination chemistry. *J Am Chem Soc* 2013;135:15443-9. [DOI](#) [PubMed](#)
60. Masa J, Zhao A, Xia W, Muhler M, Schuhmann W. Metal-free catalysts for oxygen reduction in alkaline electrolytes: influence of the presence of Co, Fe, Mn and Ni inclusions. *Electrochim Acta* 2014;128:271-8. [DOI](#)
61. Shen H, Gracia-Espino E, Ma J, et al. Synergistic effects between atomically dispersed Fe-N-C and C-S-C for the oxygen reduction reaction in acidic media. *Angew Chem Int Ed* 2017;56:13800-4. [DOI](#)
62. Li J, Zhang H, Samarakoon W, et al. Thermally driven structure and performance evolution of atomically dispersed FeN₄ sites for oxygen reduction. *Angew Chem Int Ed* 2019;58:18971-80. [DOI](#)
63. Li Y, Liu X, Zheng L, et al. Preparation of Fe-N-C catalysts with FeN_x (x = 1, 3, 4) active sites and comparison of their activities for the oxygen reduction reaction and performances in proton exchange membrane fuel cells. *J Mater Chem A* 2019;7:26147-53. [DOI](#)
64. Zhu C, Shi Q, Xu BZ, et al. Hierarchically porous M-N-C (M = Co and Fe) single-atom electrocatalysts with robust MN_x active moieties enable enhanced ORR performance. *Adv Energy Mater* 2018;8:1801956. [DOI](#)
65. Kabir S, Artyushkova K, Kiefer B, Atanassov P. Computational and experimental evidence for a new TM-N₃/C moiety family in non-PGM electrocatalysts. *Phys Chem Chem Phys* 2015;17:17785-9. [DOI](#) [PubMed](#)

66. Zhang J, Wang Z, Zhu Z. A density functional theory study on mechanism of electrochemical oxygen reduction on FeN₃-graphene. *J Electrochem Soc* 2015;162:F1262. DOI
67. Huang J, Lu Q, Ma X, Yang X. Bio-inspired FeN₅ moieties anchored on a three-dimensional graphene aerogel to improve oxygen reduction catalytic performance. *J Mater Chem A* 2018;6:18488-97. DOI
68. Zhu Y, Zhang B, Liu X, Wang DW, Su DS. Unravelling the structure of electrocatalytically active Fe-N complexes in carbon for the oxygen reduction reaction. *Angew Chem Int Ed* 2014;53:10673-7. DOI
69. Zitolo A, Goellner V, Armel V, et al. Identification of catalytic sites for oxygen reduction in iron- and nitrogen-doped graphene materials. *Nat Mater* 2015;14:937-42. DOI
70. Chung HT, Cullen DA, Higgins D, et al. Direct atomic-level insight into the active sites of a high-performance PGM-free ORR catalyst. *Science* 2017;357:479-84. DOI
71. Shen H, Gracia-espino E, Ma J, et al. Atomically FeN₂ moieties dispersed on mesoporous carbon: a new atomic catalyst for efficient oxygen reduction catalysis. *Nano Energy* 2017;35:9-16. DOI
72. Song P, Wang Y, Pan J, Xu W, Zhuang L. Structure-activity relationship in high-performance iron-based electrocatalysts for oxygen reduction reaction. *J Power Sources* 2015;300:279-84. DOI
73. Lefèvre M, Dodelet JP, Bertrand P. Molecular oxygen reduction in PEM fuel cells: evidence for the simultaneous presence of two active sites in Fe-based catalysts. *J Phys Chem B* 2002;106:8705-13. DOI
74. Li J, Sougrati MT, Zitolo A, et al. Identification of durable and non-durable FeN_x sites in Fe-N-C materials for proton exchange membrane fuel cells. *Nat Catal* 2021;4:10-9. DOI
75. Liu S, Shi Q, Wu G. Solving the activity-stability trade-off riddle. *Nat Catal* 2021;4:6-7. DOI
76. Xu X, Zhang X, Kuang Z, et al. Investigation on the demetallation of Fe-N-C for oxygen reduction reaction: the influence of structure and structural evolution of active site. *Appl Catal B Environ* 2022;309:121290. DOI
77. Liu S, Li C, Zachman MJ, et al. Atomically dispersed iron sites with a nitrogen-carbon coating as highly active and durable oxygen reduction catalysts for fuel cells. *Nat Energy* 2022;7:652-63. DOI
78. Yang L, Cheng D, Xu H, et al. Unveiling the high-activity origin of single-atom iron catalysts for oxygen reduction reaction. *Proc Natl Acad Sci USA* 2018;115:6626-31. DOI PubMed PMC
79. Wang X, Jia Y, Mao X, et al. Edge-rich Fe-N₄ active sites in defective carbon for oxygen reduction catalysis. *Adv Mater* 2020;32:e2000966. DOI
80. Liu K, Wu G, Wang G. Role of local carbon structure surrounding FeN₄ sites in boosting the catalytic activity for oxygen reduction. *J Phys Chem C* 2017;121:11319-24. DOI
81. Fu X, Li N, Ren B, et al. Tailoring FeN₄ sites with edge enrichment for boosted oxygen reduction performance in proton exchange membrane fuel cell. *Adv Energy Mater* 2019;9:1803737. DOI
82. Mineva T, Matanovic I, Atanassov P, et al. Understanding active sites in pyrolyzed Fe-N-C catalysts for fuel cell cathodes by bridging density functional theory calculations and ⁵⁷Fe Mössbauer spectroscopy. *ACS Catal* 2019;9:9359-71. DOI
83. Matter PH, Wang E, Millet JM, Ozkan US. Characterization of the iron phase in CN_x-based oxygen reduction reaction catalysts. *J Phys Chem C* 2007;111:1444-50. DOI
84. Li D, Jia Y, Chang G, et al. A defect-driven metal-free electrocatalyst for oxygen reduction in acidic electrolyte. *Chem* 2018;4:2345-56. DOI
85. Fellingner TP, Hasché F, Strasser P, Antonietti M. Mesoporous nitrogen-doped carbon for the electrocatalytic synthesis of hydrogen peroxide. *J Am Chem Soc* 2012;134:4072-5. DOI PubMed
86. Artyushkova K, Serov A, Rojas-carbonell S, Atanassov P. Chemistry of multitudinous active sites for oxygen reduction reaction in transition metal-nitrogen-carbon electrocatalysts. *J Phys Chem C* 2015;119:25917-28. DOI
87. Parvez K, Yang S, Hernandez Y, et al. Nitrogen-doped graphene and its iron-based composite as efficient electrocatalysts for oxygen reduction reaction. *ACS Nano* 2012;6:9541-50. DOI
88. Liu G, Li X, Ganesan P, Popov BN. Studies of oxygen reduction reaction active sites and stability of nitrogen-modified carbon composite catalysts for PEM fuel cells. *Electrochim Acta* 2010;55:2853-8. DOI
89. Lai L, Potts JR, Zhan D, et al. Exploration of the active center structure of nitrogen-doped graphene-based catalysts for oxygen reduction reaction. *Energy Environ Sci* 2012;5:7936-42. DOI
90. Cui X, Yang S, Yan X, et al. Pyridinic-nitrogen-dominated graphene aerogels with Fe-N-C coordination for highly efficient oxygen reduction reaction. *Adv Funct Mater* 2016;26:5708-17. DOI
91. Huang X, Wu X, Niu Y, Dai C, Xu M, Hu W. Effect of nanoparticle composition on oxygen reduction reaction activity of Fe/N-C catalysts: a comparative study. *Catal Sci Technol* 2019;9:711-7. DOI
92. Li G, Zhang J, Li W, Fan K, Xu C. 3D interconnected hierarchical porous N-doped carbon constructed by flake-like nanostructure with Fe/Fe₃C for efficient oxygen reduction reaction and supercapacitor. *Nanoscale* 2018;10:9252-60. DOI
93. Zhang SL, Guan BY, Wu HB, Lou XWD. Metal-organic framework-assisted synthesis of compact Fe₂O₃ nanotubes in Co₃O₄ host with enhanced lithium storage properties. *Nanomicro Lett* 2018;10:44. DOI PubMed PMC
94. Faubert G, Lalande G, Côté R, et al. Heat-treated iron and cobalt tetraphenylporphyrins adsorbed on carbon black: Physical characterization and catalytic properties of these materials for the reduction of oxygen in polymer electrolyte fuel cells. *Electrochim Acta* 1996;41:1689-701. DOI
95. Varnell JA, Tse EC, Schulz CE, et al. Identification of carbon-encapsulated iron nanoparticles as active species in non-precious metal

- oxygen reduction catalysts. *Nat Commun* 2016;7:12582. DOI PubMed PMC
96. Choi CH, Choi WS, Kasian O, et al. Unraveling the nature of sites active toward hydrogen peroxide reduction in Fe-N-C catalysts. *Angew Chem Int Ed* 2017;56:8809-12. DOI PubMed PMC
 97. Qiao Y, Yuan P, Hu Y, et al. Sulfuration of an Fe-N-C catalyst containing Fe_xC/Fe species to enhance the catalysis of oxygen reduction in acidic media and for use in flexible Zn-air batteries. *Adv Mater* 2018;30:e1804504. DOI
 98. Hu E, Yu XY, Chen F, Wu Y, Hu Y, Lou XW. Graphene layers-wrapped Fe/Fe₃C₂ nanoparticles supported on N-doped graphene nanosheets for highly efficient oxygen reduction. *Adv Energy Mater* 2018;8:1702476. DOI
 99. Wang Y, Gan R, Liu H, et al. Fe₃O₄/Fe₂O₃/Fe nanoparticles anchored on N-doped hierarchically porous carbon nanospheres as a high-efficiency ORR electrocatalyst for rechargeable Zn-air batteries. *J Mater Chem A* 2021;9:2764-74. DOI
 100. Kramm UI, Herrmann-Geppert I, Behrends J, Lips K, Fiechter S, Bogdanoff P. On an easy way to prepare metal-nitrogen doped carbon with exclusive presence of MeN₄-type sites active for the ORR. *J Am Chem Soc* 2016;138:635-40. DOI
 101. Wang Y, Wu M, Wang K, Chen J, Yu T, Song S. Fe₃O₄@N-doped interconnected hierarchical porous carbon and its 3D integrated electrode for oxygen reduction in acidic media. *Adv Sci* 2020;7:2000407. DOI PubMed PMC
 102. Gong K, Du F, Xia Z, Durstock M, Dai L. Nitrogen-doped carbon nanotube arrays with high electrocatalytic activity for oxygen reduction. *Science* 2009;323:760-4. DOI PubMed
 103. Zhao Y, Wan J, Yao H, et al. Few-layer graphdiyne doped with sp-hybridized nitrogen atoms at acetylenic sites for oxygen reduction electrocatalysis. *Nat Chem* 2018;10:924-31. DOI
 104. Yang L, Shui J, Du L, et al. Carbon-based metal-free ORR electrocatalysts for fuel cells: past, present, and future. *Adv Mater* 2019;31:e1804799. DOI
 105. Liu J, Song P, Xu W. Structure-activity relationship of doped-nitrogen (N)-based metal-free active sites on carbon for oxygen reduction reaction. *Carbon* 2017;115:763-72. DOI
 106. Rao CV, Cabrera CR, Ishikawa Y. In search of the active site in nitrogen-doped carbon nanotube electrodes for the oxygen reduction reaction. *J Phys Chem Lett* 2010;1:2622-7. DOI
 107. Li H, Kang W, Wang L, et al. Synthesis of three-dimensional flowerlike nitrogen-doped carbons by a copolyolysis route and the effect of nitrogen species on the electrocatalytic activity in oxygen reduction reaction. *Carbon* 2013;54:249-57. DOI
 108. Meng J, Liu Z, Liu X, et al. Scalable fabrication and active site identification of MOF shell-derived nitrogen-doped carbon hollow frameworks for oxygen reduction. *J Mater Sci Technol* 2021;66:186-92. DOI
 109. Wang N, Lu B, Li L, et al. Graphitic nitrogen is responsible for oxygen electroreduction on nitrogen-doped carbons in alkaline electrolytes: insights from activity attenuation studies and theoretical calculations. *ACS Catal* 2018;8:6827-36. DOI
 110. Liu R, Wu D, Feng X, Müllen K. Nitrogen-doped ordered mesoporous graphitic arrays with high electrocatalytic activity for oxygen reduction. *Angew Chem Int Ed* 2010;49:2565-9. DOI PubMed
 111. Kim H, Lee K, Woo SI, Jung Y. On the mechanism of enhanced oxygen reduction reaction in nitrogen-doped graphene nanoribbons. *Phys Chem Chem Phys* 2011;13:17505-10. DOI
 112. Wang J, Li L, Wei Z. Density functional theory study of oxygen reduction reaction on different types of N-doped graphene. *Acta Phys Chim Sin* 2016;32:321-8. DOI
 113. Li M, Liu Z, Wang F, Xuan J. The influence of the type of N doping on the performance of bifunctional N-doped ordered mesoporous carbon electrocatalysts in oxygen reduction and evolution reaction. *J Energy Chem* 2017;26:422-7. DOI
 114. Quílez-bermejo J, Melle-franco M, San-fabián E, Morallón E, Cazorla-amorós D. Towards understanding the active sites for the ORR in N-doped carbon materials through fine-tuning of nitrogen functionalities: an experimental and computational approach. *J Mater Chem A* 2019;7:24239-50. DOI
 115. Liu Z, Zhao Z, Wang Y, et al. In situ exfoliated, edge-rich, oxygen-functionalized graphene from carbon fibers for oxygen electrocatalysis. *Adv Mater* 2017;29:1606207. DOI
 116. Shen A, Zou Y, Wang Q, et al. Oxygen reduction reaction in a droplet on graphite: direct evidence that the edge is more active than the basal plane. *Angew Chem Int Ed* 2014;53:10804-8. DOI
 117. Tao L, Wang Q, Dou S, et al. Edge-rich and dopant-free graphene as a highly efficient metal-free electrocatalyst for the oxygen reduction reaction. *Chem Commun* 2016;52:2764-7. DOI
 118. Xue L, Li Y, Liu X, et al. Zigzag carbon as efficient and stable oxygen reduction electrocatalyst for proton exchange membrane fuel cells. *Nat Commun* 2018;9:3819. DOI PubMed PMC
 119. Ye G, Liu S, Huang K, et al. Domain-confined etching strategy to regulate defective sites in carbon for high-efficiency electrocatalytic oxygen reduction. *Adv Funct Mater* 2022;32:2111396. DOI
 120. Zhang L, Gu T, Lu K, Zhou L, Li DS, Wang R. Engineering synergistic edge-N dipole in metal-free carbon nanoflakes toward intensified oxygen reduction electrocatalysis. *Adv Funct Mater* 2021;31:2103187. DOI
 121. Kou Z, Guo B, He D, Zhang J, Mu S. Transforming two-dimensional boron carbide into boron and chlorine dual-doped carbon nanotubes by chlorination for efficient oxygen reduction. *ACS Energy Lett* 2018;3:184-90. DOI
 122. Zhao Y, Yang L, Chen S, et al. Can boron and nitrogen co-doping improve oxygen reduction reaction activity of carbon nanotubes? *J Am Chem Soc* 2013;135:1201-4. DOI
 123. Jiang H, Wang Y, Hao J, Liu Y, Li J, Li J. N and P co-functionalized three-dimensional porous carbon networks as efficient metal-free electrocatalysts for oxygen reduction reaction. *Carbon* 2017;122:64-73. DOI
 124. Gao Y, Kong D, Liang J, et al. Inside-out dual-doping effects on tubular catalysts: structural and chemical variation for advanced

- oxygen reduction performance. *Nano Res* 2022;15:361-7. DOI
125. Zan Y, Zhang Z, Dou M, Wang F. Enhancement mechanism of sulfur dopants on the catalytic activity of N and P co-doped three-dimensional hierarchically porous carbon as a metal-free oxygen reduction electrocatalyst. *Catal Sci Technol* 2019;9:5906-14. DOI
 126. Zhang H, Guang H, Li R, et al. Doping engineering: modulating the intrinsic activity of bifunctional carbon-based oxygen electrocatalysts for high-performance zinc-air batteries. *J Mater Chem A* 2022;10:21797-815. DOI
 127. Yang N, Li L, Li J, Ding W, Wei Z. Modulating the oxygen reduction activity of heteroatom-doped carbon catalysts via the triple effect: charge, spin density and ligand effect. *Chem Sci* 2018;9:5795-804. DOI PubMed PMC
 128. Pei Z, Li H, Huang Y, et al. Texturing in situ: N,S-enriched hierarchically porous carbon as a highly active reversible oxygen electrocatalyst. *Energy Environ Sci* 2017;10:742-9. DOI
 129. Guo L, Hwang S, Li B, et al. Promoting atomically dispersed MnN₄ sites via sulfur doping for oxygen reduction: unveiling intrinsic activity and degradation in fuel cells. *ACS Nano* 2021;15:6886-99. DOI
 130. Liu H, Jiang L, Wang Y, et al. Boosting oxygen reduction with coexistence of single-atomic Fe and Cu sites decorated nitrogen-doped porous carbon. *Chem Eng J* 2023;452:138938. DOI
 131. Wang Z, Jin X, Zhu C, et al. Atomically dispersed Co₂-N₆ and Fe-N₄ costructures boost oxygen reduction reaction in both alkaline and acidic media. *Adv Mater* 2021;33:e2104718. DOI
 132. Yin H, Yuan P, Lu BA, et al. Phosphorus-driven electron delocalization on edge-type FeN₄ active sites for oxygen reduction in acid medium. *ACS Catal* 2021;11:12754-62. DOI
 133. Sun Y, Sun S, Yang H, Xi S, Gracia J, Xu ZJ. Spin-related electron transfer and orbital interactions in oxygen electrocatalysis. *Adv Mater* 2020;32:e2003297. DOI
 134. Yang G, Zhu J, Yuan P, et al. Regulating Fe-spin state by atomically dispersed Mn-N in Fe-N-C catalysts with high oxygen reduction activity. *Nat Commun* 2021;12:1734. DOI PubMed PMC
 135. Li X, Chen T, Yang B, Xiang Z. Fundamental understanding of electronic structure in FeN₄ Site on electrocatalytic activity via dz₂-orbital-driven charge tuning for acidic oxygen reduction. *Angew Chem Int Ed* 2023;62:e202215441. DOI
 136. Jiang R, Li L, Sheng T, Hu G, Chen Y, Wang L. Edge-site engineering of atomically dispersed Fe-N₄ by selective C-N bond cleavage for enhanced oxygen reduction reaction activities. *J Am Chem Soc* 2018;140:11594-8. DOI
 137. Gong L, Zhang H, Wang Y, et al. Bridge bonded oxygen ligands between approximated FeN₄ sites confer catalysts with high ORR performance. *Angew Chem Int Ed* 2020;59:13923-8. DOI
 138. Shah SSA, Najam T, Yang J, Javed MS, Peng L, Wei Z. Modulating the microenvironment structure of single Zn atom: ZnN₄P/C active site for boosted oxygen reduction reaction. *Chin J Catal* 2022;43:2193-201. DOI
 139. Wang S, Borisevich AY, Rashkeev SN, et al. Dopants adsorbed as single atoms prevent degradation of catalysts. *Nat Mater* 2004;3:143-6. DOI
 140. Yin P, Yao T, Wu Y, et al. Single cobalt atoms with precise N-coordination as superior oxygen reduction reaction catalysts. *Angew Chem Int Ed* 2016;55:10800-5. DOI
 141. Li J, Chen M, Cullen DA, et al. Atomically dispersed manganese catalysts for oxygen reduction in proton-exchange membrane fuel cells. *Nat Catal* 2018;1:935-45. DOI
 142. Xin C, Shang W, Hu J, et al. Integration of morphology and electronic structure modulation on atomic iron-nitrogen-carbon catalysts for highly efficient oxygen reduction. *Adv Funct Mater* 2022;32:2108345. DOI
 143. Li Z, Leng L, Ji S, et al. Engineering the morphology and electronic structure of atomic cobalt-nitrogen-carbon catalyst with highly accessible active sites for enhanced oxygen reduction. *J Energy Chem* 2022;73:469-77. DOI
 144. Ding W, Li L, Xiong K, et al. Shape fixing via salt recrystallization: a morphology-controlled approach to convert nanostructured polymer to carbon nanomaterial as a highly active catalyst for oxygen reduction reaction. *J Am Chem Soc* 2015;137:5414-20. DOI
 145. Wan X, Liu X, Li Y, et al. Fe-N-C electrocatalyst with dense active sites and efficient mass transport for high-performance proton exchange membrane fuel cells. *Nat Catal* 2019;2:259-68. DOI
 146. Qiao M, Wang Y, Wang Q, et al. Hierarchically ordered porous carbon with atomically dispersed FeN₄ for ultraefficient oxygen reduction reaction in proton-exchange membrane fuel cells. *Angew Chem Int Ed* 2020;59:2688-94. DOI
 147. Chen Y, Kone I, Gong Y, et al. Ultra-thin carbon nanosheets-assembled 3D hierarchically porous carbon for high performance zinc-air batteries. *Carbon* 2019;152:325-34. DOI
 148. Zhang X, Zhang S, Yang Y, et al. A general method for transition metal single atoms anchored on honeycomb-like nitrogen-doped carbon nanosheets. *Adv Mater* 2020;32:e1906905. DOI
 149. Chakraborty R, K V, Pradhan M, Nayak AK. Recent advancement of biomass-derived porous carbon based materials for energy and environmental remediation applications. *J Mater Chem A* 2022;10:6965-7005. DOI
 150. Ma Z, Han Y, Wang X, Sun G, Li Y. Lignin-derived hierarchical porous flower-like carbon nanosheets decorated with biomass carbon quantum dots for efficient oxygen reduction. *Colloids Surf A Physicochem Eng Asp* 2022;652:129818. DOI
 151. Liu L, Zeng G, Chen J, Bi L, Dai L, Wen Z. N-doped porous carbon nanosheets as pH-universal ORR electrocatalyst in various fuel cell devices. *Nano Energy* 2018;49:393-402. DOI
 152. Jalalah M, Han H, Nayak AK, Hazzaz FA. Biomass-derived metal-free porous carbon electrocatalyst for efficient oxygen reduction reactions. *J Taiwan Inst Chem Eng* 2023;147:104905. DOI
 153. Wang S, Jiang H, Song L. Recent progress in defective carbon-based oxygen electrode materials for rechargeable zinc-air batteries. *Batteries Supercaps* 2019;2:509-23. DOI

154. Jia Y, Chen J, Yao X. Defect electrocatalytic mechanism: concept, topological structure and perspective. *Mater Chem Front* 2018;2:1250-68. [DOI](#)
155. Qiao Y, Kong F, Zhang C, Li R, Kong A, Shan Y. Highly efficient oxygen electrode catalyst derived from chitosan biomass by molten salt pyrolysis for zinc-air battery. *Electrochim Acta* 2020;339:135923. [DOI](#)
156. Cheng W, Yuan P, Lv Z, et al. Boosting defective carbon by anchoring well-defined atomically dispersed metal-N₄ sites for ORR, OER, and Zn-air batteries. *Appl Catal B Environ* 2020;260:118198. [DOI](#)
157. Jia Y, Zhang L, Zhuang L, et al. Identification of active sites for acidic oxygen reduction on carbon catalysts with and without nitrogen doping. *Nat Catal* 2019;2:688-95. [DOI](#)
158. Huang X, Shen T, Sun S, Hou Y. Synergistic modulation of carbon-based, precious-metal-free electrocatalysts for oxygen reduction reaction. *ACS Appl Mater Interfaces* 2021;13:6989-7003. [DOI](#) [PubMed](#)
159. He Y, Liu S, Priest C, Shi Q, Wu G. Atomically dispersed metal-nitrogen-carbon catalysts for fuel cells: advances in catalyst design, electrode performance, and durability improvement. *Chem Soc Rev* 2020;49:3484-524. [DOI](#)